Authors Response

We would like to thank the anonymous referees for their thorough review of our manuscript. Please find our responses to each of the referee's suggestions and specific comments below.

Font legend:

Referee comments

Authors response

Changed text in manuscript

Referee 1

The work is within the scope of the journal; however, the authors have to invest a bit more to provide it a clear added value. The authors used adequate procedure for sampling, handling and analyses. The manuscript reports highly impressive number of sampling points and various hydrochemical parameters. It clearly presents a valuable data set. However, the need for such a dataset should be clearly explained and justified. As a minimal starting point in the Introduction, please explain the difference (and novelty) of this work compared to data available from Partners/Arctic GRO at this river terminal gauging station.

Thank you very much for your review of our manuscript. Regarding the justification for the need of such a dataset, we have added a sentence into the introduction:

"Understanding the impact of climate shifts requires a high-quality, high-frequency dataset to assess current conditions and predict future trends."

In multiple sentences in the conclusion, we detail ways in which the scientific utility of the dataset is justified. Other than that, we think there is sufficient justification already in the introduction for such a dataset as the one that we present. Here a few examples from our introduction that serve as a justification for the need of this dataset: a) "There is no paleo-historical analogue for these changes, therefore, establishing a baseline of current fluxes and understanding how the system is changing are

necessary to anticipate the scope and consequence of future impacts of climate warming and permafrost thaw."; b) "To understand the changes underway, their impacts on the river system and, in turn, their impacts on the global climate, a baseline of observations that includes biogeochemistry is required. It is a prerequisite for deriving improved insights into linkages between land and ocean and between river system and climate that will allow for better constraining future impacts of continued warming."; c) "Higher sampling frequency can improve annual flux estimates, as does dedicated sampling over the whole hydrological cycle. Arctic rivers are typically characterized by a nival hydrological regime, and, thus, the strong seasonality and high variability in summer water balance may mandate high-frequency data collection, especially during the highly dynamic shoulder seasons (freshet, freeze-up)."; d) "In addition, higher frequency or even continuous in situ measurements (e.g., Castro-Morales et al., 2022) will create new opportunities to validate remotely sensed data (El Kassar et al., 2023) or model results (e.g. Rawlins and Karmalkar, 2024) and to potentially upscale data spatially."

In the main text and figures, the authors should provide a comparison with data of ARCTIC GRO/Partners obtained at the Kysur gauging station. Appendix D is just great, but it should be in the main text. Other measured parameters (those available from ArcticGRO) should be shown as well.

We moved the figures of the Appendix D to the main manuscript (replaced the old ones with the one containing ArcticGRO data) and added a few sentences comparing the data. In addition, we added the remaining parameters that are sampled by ArcticGRO and our program for a direct comparison (temperature, DOC and CDOM, TDN, several ions). Consequently, we removed Appendix D.

We added a sentence to the methods:

"In addition to the data sampled at Samoylov Island, we included data from the ArcticGRO program for all parameters that were measured by both programs (temperature, DOM, nutrients, ions)."

as well as description to the results:

"DOC and aCDOM(254) generally agrees with data from ArcticGRO sampled several hundreds of km further upstream, however it shows a generally lower DOC to aCDOM(254) ratio compared to our data."

"Comparing TDN, Si, NH4, and NO3 with data from ArcticGRO reveals a good agreement between the datasets."

"We compared some of the dissolved elemental and ion concentrations with those measured by the ArcticGRO program, which shows a generally good agreement. Some stronger differences might be related to the earlier arrival of changing seasons at the ArcticGRO sampling location further south."

We also added the ArcticGRO description to the figure captions.

The authors possess both discharges and concentrations. Export fluxes (via, for example, LOADEST or any other mean) should be calculated and compared with earlier fluxes. It is the duty of the authors to provide the fluxes, the readers cannot do it themselves. Within the concept of this journal, I assume no discussion of concentration dependence on the discharge and comparison with other rivers are needed. However, the export fluxes (mean multi-annual values or yields) should be there.

Thank you for these suggestions to calculate and report fluxes. We do report the selected parameter fluxes from this dataset in research papers some of which are already published. See e.g. DOC and CDOM fluxes in Juhls et al. 2020 (https://www.frontiersin.org/articles/10.3389/fenvs.2020.00053/full), seasonal and interannual DOC fluxes from multiple years compared with satellite-derived fluxes in El Kassar et al., 2023 (https://www.frontiersin.org/journals/marine-science/articles/10.3389/fmars.2023.1082109/full), and nutrient fluxes in Sanders et al., 2021 (https://link.springer.com/article/10.1007/s13280-021-01665-0). We also refer to these papers in the manuscript. While we have additional publications in preparation that will cover annual and seasonal biogeochemical fluxes, we believe this is beyond the scope of ESSD for this manuscript due to methodological considerations in flux calculation. For example, although the load models such as LOADEST are commonly used for estimating fluxes, we find it less suitable for capturing seasonal or long-term fluxes influenced by non-linear processes, such as permafrost thaw, where no consistent relationship between discharge and concentration of biogeochemical parameters exists. To address such complexities, we prioritize high-frequency sampling, which allows for direct linear interpolation between sampling days for daily flux calculations. Currently, we are working on a research paper manuscript that shows differences between load-models trained with a low number of samples per year

and a high-frequency sampling program. It is critical that data-users match their flux calculation methods to the purpose for which the fluxes are calculated.

Specific issues:

L90-91 Please note that annual fluxes of most solutes in Arctic rivers can be reasonably (within 20-30 %, which is lower than annual inter-variations) can be approximated by July-August sampling (see for instance https://doi.org/10.1016/j.chemgeo.2022.121180)

Thank you for this note. We do not fully agree with the statement that "most" solutes can be reasonably estimated due to their robust relationship with discharge. The study by Pokrovsky et al., 2022 also shows that there are multiple groups of solutes and biogeochemical parameters that have differently robust or have no relationship to discharge.

L 190-191 This is certainly a valid explanation

Great to hear.

L461-463 I certainly agree with this statement

Great to hear.

L473-474 Here I also completely agree with authors' statement. Great and very timing work, badly needed for world scientific community.

Great to hear. We are happy that the need for this dataset became apparent by reading the manuscript. By adding another sentence to the introduction, we hope that you now agree that it will also become apparent at the beginning of the manuscript.

Fig. A1: The dates should be shown on these graphs

Good suggestion! We indicated the dates on the CTD profiles by coloring the lines and adding a legend.

Fig. B2: Comparison of two method of sample treatment for analyses is very useful. It is a pity that no "filtered and frozen" method was tested, because this technique is certainly the best for adequate assessment of nutrients

Please note that Figure B2 shows the comparisons for selected parameters using two protocols but the same analytical method. Dissolved inorganic nutrients as presented in Figure 12 are "filtered and frozen" following the most common protocols. We added a sentence to the Appendix B to clarify what parameters were compared:

"For a set of samples covering the period from 13 September 2019 to 2 May 2020, we measured the electrical conductivity (Fig. B1), major ion concentrations (Fig. B2), and dissolved elemental concentrations (Fig B3) measured as described in Table 1 but with two different protocols to assess the impact of sample processing on the dissolved elemental and ion concentrations."

p.34, Fig. B3: The data on P are unclear – what do negative values mean?

This is correct, the negative concentrations have no physical significance. They reflect the detector response after calibration. Please note that all values shown here are below our detection limit indicated in Table 1 and in Figure 14. For full transparency, we decided to show these data anyways, always reporting the detection limit for potential user applications.

It is clear that for analyses of Fe, Ca, Ba, Al, on site filtration is mandatory prior to analyses. Please make sure you let it express in the text, because this is very important finding

We would like to clarify that on-site filtration for Fe, Ca, Ba, and Al was performed only for the subset of samples highlighted in green in Figure B1. For all other samples, they were frozen immediately after collection and later thawed and filtered in the lab prior to analysis. A protocol change occurred after sample #077 regarding the handling of dissolved elemental and ion concentrations (see Table 1). Specifically, samples #001 to #077 were transported unfrozen, while samples numbered >#077 were transported frozen. In Figure 14a, a noticeable offset is observed between samples <77 and >77 for Al, with the unfrozen transported samples (<77) showing lower concentrations than the frozen transported samples (>77). This mirrors the effect seen in Appendix B, where frozen and unfrozen samples from the

same set were compared. Therefore, we speculate that the observed differences are more likely due to the impact of freezing versus non-freezing rather than the timing of filtration (whether performed on-site or post-transport). To definitively determine whether the filtration timing or freezing is the primary factor causing these differences, however, a split-sample approach with both processing methods would be necessary for future assessments.

We added some more description to the results:

"The different protocol (transport of samples cooled vs transport of samples frozen) between samples <#077 and >#077 resulted in visible offsets between the sample sets (i.e., F, Al, Mn, ..). The differences between unfrozen and frozen samples across different sample sets seem similar to those shown in Appendix B (comparing frozen and unfrozen samples of the same sample set)."

Referee 2:

General Comments:

This is a very valuable contribution. The existence and maintenance of such sustained sampling and measurement programs of physical and biogeochemical parameters of river systems is of paramount importance given the integrative nature of the information rivers carry about the corresponding watersheds, their role in linking terrestrial and marine environments and ecosystems, and their ability to reveal system-wide change. Such initiatives are of particular importance for regions of the planet that are experiencing accelerated change, such as the Arctic, where information can be used to gauge biogeochemical, and ecological responses to changing hydrological and climate conditions. Furthermore, the fate of the vast stores of carbon currently residing in permafrost in the face of on-going warming and hydrological change underlines the significance of this region in terms of global climate. With the unprecedented pace of change underway, there is the urgent need for comprehensive and intensive observation programs that provide context for this change.

Fortunately, the biogeochemistry of the major Arctic rivers have been the focus of sustained observations as a consequence of programs such as the pan-Arctic River sampling programs (PARTNERS) and Arctic Great Rivers Observatory (ArcticGRO) which extent back more than 20

years. However, these programs have been characterized by low temporal resolution, with large data gaps, particularly for specific seasons and transitional periods (shoulder seasons of freshet & freeze-up) rendering it hard to investigate different processes and constrain shorter-term variability. In such circumstances, the authors correctly highlight the limitations of models as an approach to bridge data gaps, and argue for the need for high-frequency measurements to better constrain flux estimates, and investigate short-term variability resulting from changes in hydrologic pathways and other phenomena. The articulated need for baseline observations is clear, although it is evident that marked changes are already upon us.

This present study describes a diverse suite of data acquired over a 4.5-year period from sampling at a station in the delta of the Lena River, one of the largest Arctic rivers, with a catchment dominated by permafrost. The 4+-year period covers a time interval during which winter discharge that is higher than the long-term average, and captures both record low and record high intervals of summer discharge. High-frequency (daily to weekly) sampling resulting in a total of almost 600 sampling dates, focussing exclusively on dissolved parameters. Acquisition of such detailed and long-term datasets always represents a compromise given logistical constraints associated with ease of sampling, sampling methods and volumes, sample storage and shipment, instrumental techniques, performance and reliability, and range of parameters sought, and of course cost. Clearly, a great deal of thought and care, as well as pragmatism, has gone into the design and execution of this high-resolution sampling program. Despite some apparent limitations and inconsistencies in the dataset the existence of such high-resolution, extended datasets remains rare, and yet is of crucial value. It is not surprising for such a long-term, multi-institution and logistically challenging endeavor focused on a remote location that the datasets are somewhat heterogeneous with respect to sample processing, storage and shipment, as well as where and how the measurements were made, with some resulting patchiness in data quality. However, the manuscript benefits from a detailed description of the methods used, and discussion is provided concerning changes in methodology over the course of the observation period, which are also indicated in the figures. Analytical uncertainties in the measurements are also provided (in Table 1). For parameters where there is significant data scatter associated with measurement on specific instruments and different laboratories, and the authors caution use and interpretation of such data where

this is evident (e.g., SUVA and SR in Figure 7; nutrients in Figure 11). In general, I think such discussions of data quality are satisfactory.

Thank you for your thorough and thoughtful review. We are grateful for your recognition of the importance of sustained high-frequency sampling programs, particularly in regions experiencing rapid environmental changes like the Arctic. As you noted, the integrative nature of rivers as conveyors of information from their watersheds to marine systems makes such programs crucial for understanding biogeochemical and ecological responses to climate and hydrological changes. We appreciate your acknowledgment of the logistical and methodological challenges inherent in collecting high-resolution data from remote Arctic locations, and your recognition of the value of our dataset despite these constraints. We agree that the variability in sample processing, storage, and shipment, as well as the multi-institutional nature of the program, have introduced some heterogeneity to the data. However, we have strived to be transparent in our methodology and have provided detailed discussions on the quality of the data, along with analytical uncertainties, as highlighted in your review. Your specific mention of our handling of data scatter and measurement inconsistencies in the manuscript, particularly regarding SUVA, SR, and nutrients, is greatly appreciated. We have been cautious in interpreting these datasets and have clearly indicated areas where uncertainty may impact the results. We are pleased that you found our discussions around data quality to be satisfactory.

What was less clear is whether efforts were made to analyze splits of the same samples for the same parameters in different labs in order to address inter-lab data comparability (i.e., beyond measurement of standards). It seems that sample batches were processed in serial fashion by only one lab or another. Clarification of this point for the different parameters would be helpful. I note that in some cases comparisons were made for the same samples that were frozen versus unfrozen (Appendix B1), but what about splits of the same sample treated in the same way, but measured by different methods/research groups? One example is the water (oxygen and hydrogen) isotope data, which were obtained by mass spectrometry and optical spectroscopy. The Lena river can exhibit quite high DOM concentrations (DOC up to 20 mg L-1), which can influence spectroscopic properties. Was there any systematic comparison of water isotope data for splits of Lena water samples (not standards) between

MS and CRDS methods? Irrespective, the transition in instrumental methods used in the measurement of specific parameters is indicated in the Figures, which is very helpful (e.g., water isotopes in Figure 5; DOC concentrations and absorbance in Figure 6).

Thank you for raising this important point. We acknowledge the need to clarify the efforts made to assess inter-laboratory data comparability beyond the use of standards. In this study, sample batches were primarily processed in serial fashion by different labs for different parameters, and we did not systematically analyze splits of the same sample across different labs for the same parameters. The logistical and financial effort that would be required precluded such tests. However, we did perform some comparisons for the same samples under different conditions, such as frozen versus unfrozen treatments (as shown in Appendix B1). We added a sentence to the conclusion recommending such tests in the future to improve comparability:

"Further, to improve inter-lab comparability, we recommend designated tests to measure splits of samples for the same parameters but in different labs and or using different protocols or instruments."

The data reveals some interesting contrasts for the same parameter but measured using different measurement methods (e.g., colorometric versus ion chromatographic determination of silicon concentrations; e.g., Fig. 12a) as well as different sampling handing protocols (e.g., electrical conductivity; cf. Appendix B). Such contrasts and systematic biases are to be expected given logistical challenges in operating such a sustained measurement program. Although such offsets/biases are not optimal, the overall density of data holds promise for the potential to anticipate and correct deviations between sample suites processed and analyzed in different ways. I think these data are also highly informative for other researchers who may be applying/developing protocols for sample collection, processing and storage. Overall, I think the manuscript provides an objective assessment of the data quality and highlights key features that emerge over the time series.

Thank you very much for your review of our manuscript describing the dataset. We agree that these systematic biases, while inevitable given the logistical constraints of a sustained Arctic sampling program, do not detract from the dataset's value. In fact, as you pointed out, the density and breadth of our data allow for robust assessments and, where necessary, corrections between sample suites

processed differently. We also appreciate your recognition of the dataset's potential as a resource for other researchers refining protocols for sample handling and storage in challenging environments. It is important to us to be transparent about possible limitations of the dataset that result from the unavoidable inconsistencies in sample handling and analyses. Your insights into the manuscript's objective assessment of data quality encourage us to continue refining our approaches and sharing these learnings for the benefit of the broader research community. Thank you again for your supportive comments.

Specific comments:

- For the DOC radiocarbon data, presumably DOC concentration data is also obtained from the elemental analyzer-MICADAS AMS measurement? If so, how did DOC concentrations compare with corresponding measurements using the more conventional DOC method (high-temperature catalytic oxidation)?

DOC concentration data is not routinely obtained during radiocarbon measurements. The Elemental Analyzer used is uncalibrated; instead, CO_2 evolved from sample combustion can be quantified manometrically using the GIS system before injection into the AMS ion source.

- Appendix D. I am glad that the authors drew a comparison between their observations and those reported by the ArcticGRO program (albeit at a more upstream location), however, I think that this would be good to include in the main body of the manuscript as I am sure this comparison will be of direct interest to the reader. Moreover, Figure D1 and D2 clearly shows the merit of performing high temporal resolution sampling and measurement in order to constrain (sub-)seasonal variability. It would be helpful to list which measured parameters (beyond DOC concentration and CDOM absorption) are covered by both the ArcticGRO and the present 4.5-year time series.

Thank you for this suggestion. Please see above the very similar suggestion by referee 1. We moved Appendix D to the main manuscript and added all other parameters that were measured by both programs for a comparison. We listed those parameters in the method section.

- A key question that could perhaps be addressed by the authors (at the end of the Discussion or in the Conclusions section) is whether, based on their findings, all parameters need to be measured with the same sampling frequency (given observed variability). In other words, can the data presented can be used to develop a recommended protocol for future, more streamlined sampling. For example, are there specific parameters that appear to be most diagnostic of specific (changes in) processes that are not captured in low-resolution datasets? Given the challenges (and costs) associated with sustaining such a sampling/measurement program, it might be helpful to consider things from a strategic point of view. Furthermore, would a repeat intensive phase of high-resolution sampling/measurements spanning a similar time interval be worth undertaking a decade from now? This may be particularly pertinent as I suspect maintaining this program given the current geopolitical situation will be challenging.

Specific recommendations about necessary sampling frequency for different parameters strongly depend on the question that one wants to answer and would require a tailored analysis that would be beyond the scope of this paper. We agree that this dataset might be used to answer these questions or to design sampling strategies for other sites. In the context of rapidly changing discharge, seasonality and long-term groundwater flow pathways, the goal of such monitoring must be to detect departures from predictable behavior, and emerging new relationships between observed parameters. We added a sentence to the conclusion:

"Using this dataset as a baseline, it should be the goal to repeat such sampling in the future, either as ongoing monitoring, or a repeated intense 4-year period. Future studies could utilize insights from this high-frequency sampling to determine the optimal sampling frequency needed to address specific scientific questions."

- Is any of the sampled material archived for future (repeat or new) measurements? If so, this should be mentioned.

Good point. We added a sentence to the "Data availability" section:

"Remaining sample volumes of analyzed samples are archived at the AWI in Potsdam, Germany."

Lena River biogeochemistry captured by a 4.5-year high-frequency sampling program

Bennet Juhls[1], Anne Morgenstern[1], Jens Hölemann[2], Antje Eulenburg[1], Birgit Heim[1], Frederieke Miesner[1,3], Hendrik Grotheer[4,5], Gesine Mollenhauer[4,5], Hanno Meyer[1], Ephraim Erkens[1,6], Felica Yara Gehde[1], Sofia Antonova[1], Sergey Chalov[7,8], Maria Tereshina[7], Oxana Erina[7], Evgeniya Fingert[7], Ekaterina Abramova[9], Tina Sanders[10], Liudmila Lebedeva[11], Nikolai Torgovkin[11], Georgii Maksimov[12], Vasily Povazhnyi[13], Rafael Gonçalves-Araujo[14], Urban Wünsch[14], Antonina Chetverova[13,15], Sophie Opfergelt[16], Pier Paul Overduin[1]

[1]Permafrost Research, Alfred Wegener Institute Helmholtz Centre for Polar and Marine Research, Potsdam, 14473, Germany
[2]Physical Oceanography of Polar Seas, Alfred Wegener Institute Helmholtz Centre for Polar and Marine Research, Bremerhaven, 27570, Germany
[3]Department of Geosciences, University of Oslo, Oslo, 0316, Norway
[4]Marine Geochemistry, Alfred Wegener Institute Helmholtz Centre for Polar and Marine Research, Bremerhaven, 27570, Germany
[5]MARUM - Center for Marine Environmental Sciences and Faculty of Geosciences, University of Bremen, Bremen, 28359, Germany
[6]Institute for Geosciences, University of Potsdam, Potsdam, 14476, Germany
[7]Faculty of Geography, Department of Hydrology, Lomonosov Moscow State University, Moscow, 129626, Russia
[8]Institute of Ecology and Environment, Kazan Federal University, Kazan 420097, Russia
[9]Lena Delta Nature Reserve, Tiksi, 678400, Sakha Republic, Russia
[10]Department of Aquatic Nutrient Cycles, Institute of Carbon Cycles, Helmholtz Centre Hereon, Geesthacht, 21502, Germany
[11]Laboratory of Permafrost Groundwater and Geochemistry, Melnikov Permafrost Institute, Russian Academy of Sciences, Yakutsk, 677010, Russia
[12]Laboratory of General Geocryology, Melnikov Permafrost Institute, Russian Academy of Sciences, Yakutsk, 677010, Russia
[13]Otto Schmidt Laboratory for Polar and Marine Research, Arctic and Antarctic Research Institute, St. Petersburg, 199397, Russia
[14]Section for Oceans and Arctic, National Institute of Aquatic Resources, Technical University of Denmark, Lyngby, 2800, Denmark
[15]Institute of Earth Science, St. Petersburg University, St. Petersburg, 199034, Russia
[16]Earth and Life Institute, Université catholique de Louvain, Louvain-la-Neuve, 1348, Belgium

Correspondence to: Bennet Juhls (bennet.juhls@awi.de)

Abstract. The Siberian Arctic is warming rapidly, causing permafrost to thaw and altering the biogeochemistry of aquatic environments, with cascading effects on the coastal and shelf ecosystems of the Arctic Ocean. The Lena River, one of the largest Arctic rivers, drains a catchment dominated by permafrost. Baseline discharge biogeochemistry data is necessary to understand present and future changes in land-to-ocean fluxes. Here, we present a high-frequency, 4.5-year-long dataset from a sampling program of the Lena River's biogeochemistry, spanning April 2018 to August 2022. The dataset comprises 587 sampling events and measurements of various parameters, including water temperature, electrical conductivity, stable oxygen and hydrogen isotopes, dissolved organic carbon concentration and ^{14}C, coloured and fluorescent dissolved organic matter, dissolved inorganic and total nutrients, and dissolved elemental and ion concentrations. Sampling consistency and continuity

and data quality were ensured through simple sampling protocols, real-time communication, and collaboration with local and international partners. The data is available as a collection of datasets separated by parameter groups and periods at https://doi.org/10.1594/PANGAEA.913197 (Juhls et al., 2020b). To our knowledge, this dataset provides an unprecedented temporal resolution of an Arctic river's biogeochemistry. This makes it a unique baseline on which future environmental changes, including changes in river hydrology, at temporal scales from precipitation event to seasonal to interannual, can be detected.

1 Introduction

River-borne organic material and nutrients influence biogeochemical processes in Arctic estuaries, coastal waters, shelf seas and, on a larger scale, the entire Arctic Ocean. The Arctic is warming nearly four times faster than the rest of the world (Rantanen et al., 2022), changing ecosystems, the intensity of geomorphic processes and aquatic biogeochemistry within river catchments. These changes are reflected in the flux of matter borne by rivers to the sea. For example, as air temperatures rise, permafrost thaws (Biskaborn et al., 2019), mobilizing and releasing organic matter and nutrients into the aquatic system (Mann et al., 2022; Vonk et al., 2019), changing hydrological pathways (Rawlins and Karmalkar, 2024) and the nature of the organic material transported (Starr et al., 2024). There is no paleo-historical analogue for these changes, therefore, establishing a baseline of current fluxes and understanding how the system is changing are necessary to anticipate the scope and consequence of future impacts of climate warming and permafrost thaw. The Lena River is the second largest Arctic river by total annual discharge, and its catchment is one of the most rapidly changing in the Arctic (Tananaev and Lotsari, 2022). The consequences of rapid warming are evident in the Lena River's hydrology. Total annual discharge is increasing (Shiklomanov et al., 2020; Tananaev et al., 2016) and the hydrological regime is shifting towards earlier freshets and later freeze-ups (Gelfan et al., 2017; Yang et al., 2002). The seasonal variability of water sources supplying the Lena River is also changing as a result. For example, winter under-ice flow has been increasing for almost the entire ~~the~~ past century (Liu et al., 2022). Such changes inevitably affect the river's biogeochemistry (Juhls et al., 2020a). The timings of river ice melt and freeze-up are undergoing significant alterations (Shiklomanov and Lammers, 2014), shifting water-atmosphere heat and mass transfer as the ice-free season lengthens. These changes are reflections of synoptic shifts in climate, which also affect the catchment and the ecosystem function of the river. Shifts in the Lena River biogeochemistry will lead to further changes in the region's climate dynamics and to currently unknown impacts on coastal ecosystems. The Lena River plays a crucial role in the global carbon cycle, transporting large amounts of organic matter from the terrestrial environment to the Arctic Ocean (e.g., Raymond et al., 2007; Semiletov et al., 2011). The Lena River also transports nutrients to shallow shelf and coastal regions, where they are important for the primary production of associated ecosystems (Terhaar et al., 2021). Riverine dissolved inorganic carbon (DIC) and dissolved organic carbon (DOC) fluxes drive outgassing of greenhouse gasses in the river plume (Bertin et al., 2023), providing one example of a feedback mechanism between changing riverine fluxes and the climate system. Rivers act not only as conveyor belts, but also transform the material they transport and represent important habitats. Food and transportation security

are two of the important ecosystem services the Lena River provides to northern communities. To understand the changes underway, their impacts on the river system and, in turn, their impacts on the global climate, a baseline of observations that includes biogeochemistry is required. It is a prerequisite for deriving improved insights into linkages between land and ocean and between river system and climate that will allow for better constraining future impacts of continued warming. The majority of studies that investigate recent Arctic fluvial biogeochemistry trends (Holmes et al., 2012; Raymond et al., 2007; Tank et al., 2023; Wild et al., 2019) are based on the series of pan-Arctic River sampling programs PARTNERS (2003–2007), Student Partners (2004-2009) and ArcticGRO (since 2009). They systematically cover the six largest Arctic rivers in respect to their discharge, including the Lena River. These programs have produced data over more than two decades, providing ~7 samples per year from each river to cover seasonal changes. Other studies investigate Lena River biogeochemistry with datasets from distinct field campaigns at specific locations or along transects (Cauwet and Sidorov, 1996; Hölemann et al., 2005) and its transport of sediment (Fedorova et al., 2015; Ogneva et al., 2023; Rachold et al., 1996), carbon (Juhls et al., 2020a; Kutscher et al., 2017; Winterfeld et al., 2015) and nutrients (Lara et al., 1998; Sanders et al., 2022). Most of these studies focus on a selected set of parameters for specific research questions and include only the summer or the open water period. Especially the shoulder season with the freshet in spring and the freeze-up in fall are mostly unstudied. Poor temporal resolution and coverage of sampling had to be bridged with models that relate discharge with biogeochemical concentrations (e.g., Holmes et al., 2012; Raymond et al., 2007; Tank et al., 2023). The necessity to use these relationships, which are often weak, can be obviated through higher frequency sampling. Juhls et al., (2020a) compare the effect of calculating annual fluxes using data sets of varying sampling frequency. Higher sampling frequency can improve annual flux estimates, as does dedicated sampling over the whole hydrological cycle. Arctic rivers are typically characterized by a nival hydrological regime, and, thus, the strong seasonality and high variability in summer water balance may mandate high-frequency data collection, especially during the highly dynamic shoulder seasons (freshet, freeze-up). Even more importantly, the assumption of correlations between biogeochemical parameters and river discharge may mask emerging catchment or river processes that are not tied to discharge. A relevant example of this are shifts in hydrologic pathways due to climate change and permafrost thaw (Prokushkin et al., 2019), which may affect organic matter (OM) quality, but not discharge (Frey and Smith, 2005). In addition, higher frequency or even continuous in situ measurements (e.g., Castro-Morales et al., 2022) will create new opportunities to validate remotely sensed data (El Kassar et al., 2023) or model results (e.g. Rawlins and Karmalkar, 2024) and to potentially upscale data spatially. The biogeochemistry of a river is impacted by environmental processes of its entire upstream catchment and may therefore reflect changes across a range of scales (Holmes et al., 2012). In order to record future changes in the Lena River biogeochemistry that are related to climate warming, it is crucial to compare new data with a baseline. Understanding the impact of climate shifts requires a high-quality, high-frequency dataset to assess current conditions and predict future trends. In this study, we present biogeochemical data collected from water sampled in the central Lena River Delta over more than four years, along with detailed descriptions of the sampling, processing and analytical methods for each parameter.

2 Study area, climatological and hydrological conditions

The Lena River stretches from the Baikal Mountains to the Laptev Sea where it forms the largest Arctic Delta. The Lena River has a total length of about 4,294 km and an average annual discharge of 689.1 km^3 $year^{-1}$ (Mann et al., 2022). More than 90 % of its catchment (2.61 x 10^6 km^2) is underlain by continuous or discontinuous permafrost (Obu et al., 2019). The two major tributaries to the Lena are the Viluy River, from the west, and the Aldan River, from the east (Fig. 1a).

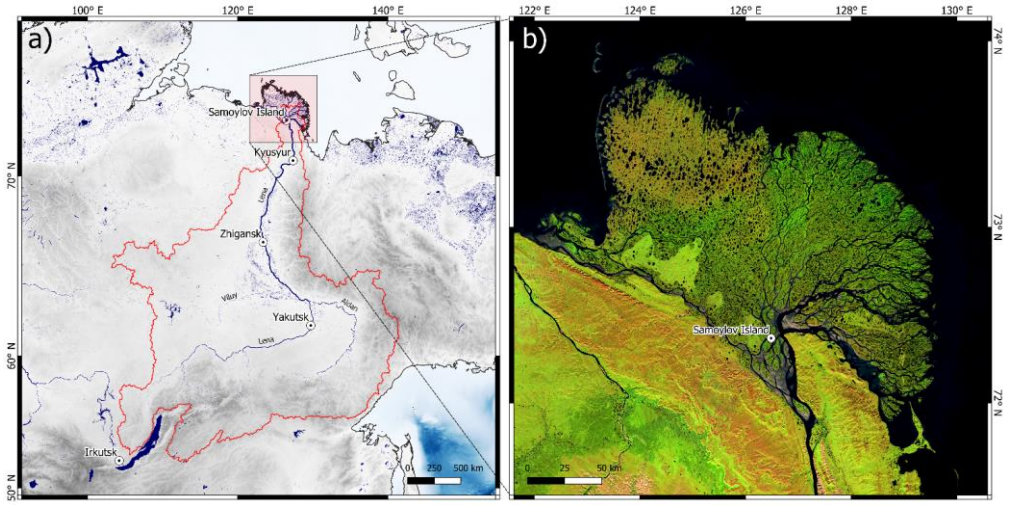

Figure 1: (a) Overview of the Lena River watershed, which is delineated by red line. Grey colours show topography, blue colours rivers, lakes and seas; (b) satellite image of the Lena River Delta with the sampling location at Samoylov Island.

The Lena River catchment is one of the coldest regions on Earth with average air temperatures below -30 °C from December to February in most years. Only for five months in the year (May to September) mean air temperatures are above 0 °C. The catchment climate is characterized by a dry winter, and most of the annual precipitation occurs during the summer months (Fig. 2). During the period covered by the sampling program in this study, the mean monthly air temperature was mostly above the long-term average (1950-2022). The precipitation for these years was mostly higher than the long-term average (1950-2022) during the winter months, but very variable during the summer months, including record low (in August 2020 and October 2022) and record high (in March 2020 and August 2022) monthly precipitation.

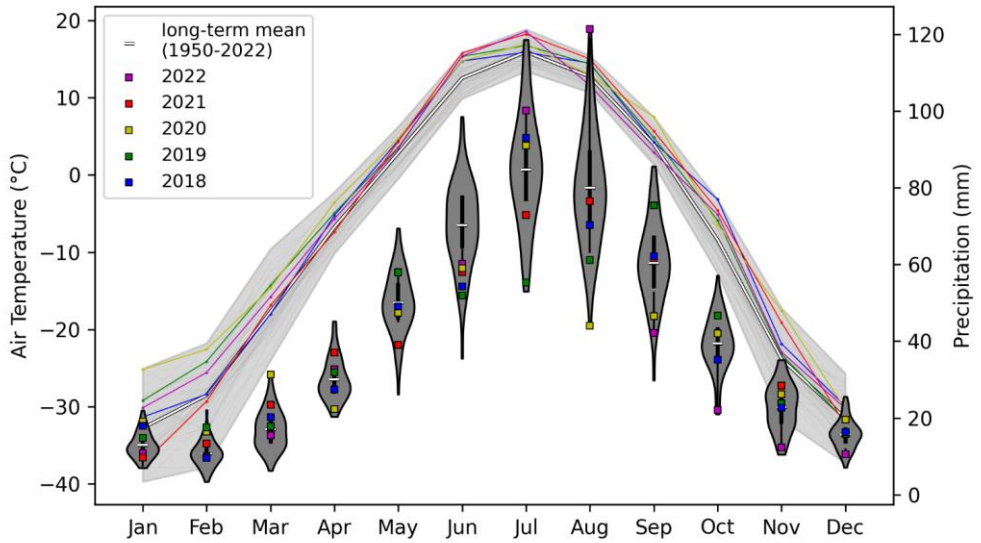

Figure 2: ERA5-land monthly mean air temperature and total precipitation for the Lena River catchment. Lines show the air temperatures, where the light gray area indicates the min-max range of all years from 1950 to 2022. Precipitation is shown by violins, where the width indicates the occurrence frequency within the years from 1950 to 2022. The years 2018 to 2022 are highlighted by colored lines (temperature) and squares in violins (precipitation). Data source: ERA5. Credit: Copernicus Climate Change Service/ECMWF

The Lena River is characterized by a nival hydrological regime with a strong discharge peak during the snowmelt and river ice break-up between the end of May and the beginning of June, a variable discharge in summer, and low base flow discharge in winter (Fig. 3, 4a). Daily discharge is monitored by the Russian Federal Service for Hydrometeorology and Environmental Monitoring (Roshydromet). All 4 years covered by the sampling program described in this study showed higher than average winter discharge, but ranged from record low to record high summer discharge. While 2018 was the year with the fourth highest annual discharge on record (1936 to 2022), 2019 was one of the driest years (ninth on record).

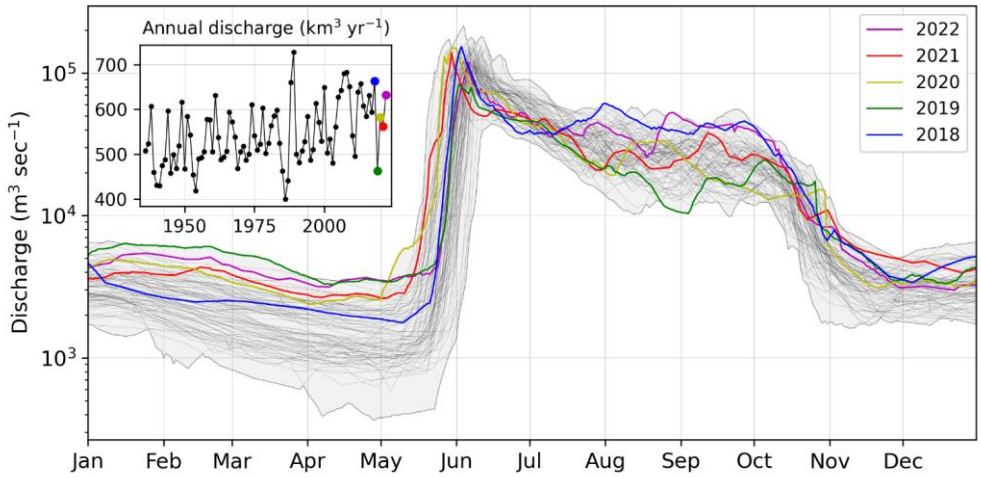

Figure 3: Discharge of the Lena River for all years from 1937 to 2022 (thin black lines) measured at Kyusyur. The years 2018 to 2022 are highlighted in colours. Grey area shows the absolute minimum and maximum for each day from 1937 to 2022. Inset figure (top left) shows the annual discharge fluxes.

3 Data Collection

The dataset is derived from a high-frequency sampling program at the Research Station Samoylov Island in the central Lena River Delta (Fig. 1b), a permanently staffed research station since 2013. It relied on the support of the non-scientific station staff and was thus designed as robust and time efficient under all seasonal conditions as possible. The exact location of sampling was the Olenekskaya Channel, south-west of Samoylov Island. The sampling location is also directly connected to the near main Lena River channel (~7 km upstream). Only surface samples were taken, and most samples were taken from the center of the channel from a boat (in summer) or through an ice hole (in winter). No stratification can be observed in the Lena River (Fig. A1), suggesting homogeneously distributed dissolved water chemistry across the water column. During ice break-up and ice freeze-up, samples were taken from the shore for safety reasons during unstable river ice conditions. The sampling started on 20 April 2018 and lasted until 16 August 2022. Throughout the first year of sampling (18 April 2018 to 6 April 2019), a sample was taken every 4 days. Between 10 May ~~to~~ and 14 June each following year, a sample was taken every day, between 15 June to 31 October every 2 days, and between 1 November to 9 May once a week. For each sampling event, 1 L of surface water was taken in a Nalgene plastic bottle pre-rinsed with river water, and the temperature was measured directly in the river using a hand-held conductivity meter. The water sample was then immediately subsampled, filtered, and conserved in the laboratory of the research station. Additionally, time of sampling, exact location (center of channel or shore), and weather

and river conditions were noted. Except for the in situ temperature measurement, all biogeochemical analyses were done after storage and transport to laboratories in Russia, Germany, and Denmark. As a result, some samples were stored up to half a year before analysis. After initial processing, samples were stored in refrigerators (+4°C) and freezers (-18°C) at the Research Station Samoylov Island until transport via Tiksi to Yakutsk, from where they were shipped to the individual labs. Dates separating sample sets (with distinct transport and analysis dates) are indicated by the dashed lines in the individual figures for each parameter. The dataset contains data from 587 sampling dates. This sampling program focuses on biogeochemical parameters, which allow a simple processing protocol to be sampled and processed by a non-scientist after initial training. It includes biogeochemical parameters mostly in the dissolved phase and excludes parameters measured on particles, because, in contrast to dissolved concentrations the river channel at Samoylov Island might not be assumed representative for the main Lena River for particulates concentrations due to their strong heterogeneity (Chalov and Prokopeva, 2021). During the first days of the spring freshet, which are accompanied by ice jams and pooling of snow and ice melt water, representative sampling of Lena River water is challenging if not impossible. Consequently, the samples during these periods can show biogeochemical signatures of dilution and need to be interpreted with caution. In addition to the data sampled at Samoylov Island, we present data from the ArcticGRO program for all parameters that were measured by both programs (temperature, DOC, CDOM, TDN, Silicon, Ammonium, Nitrate, Barium, Calcium, Potassium, Magnesium, Sodium, Strontium, Sulphate, Chloride, Fluoride). The periods of ice cover on the Lena River were visually estimated using daily MODIS imagery (https://worldview.earthdata.nasa.gov/) and shown by the white (ice-covered) and grey (ice-free) backgrounds in the individual figures for each parameter. Table 1 provides an overview of the sample processing and analysis methodology for each biogeochemical parameter and each set of samples.

Table 1: Overview of sample processing and analysis for each group of parameters for each set of samples.

Parameter	Period / Sample ID	Sample processing	Method, Instrument, Location	Accuracy/Error
Temperature	20 Apr 2018 (#001) to 16 Aug 2022 (#612)	in situ measured	Handheld conductivity meter (WTW COND 340i), in situ	±0.5 %
Electrical conductivity (EC)	20 Apr 2018 (#001) to 6 Apr 2019 (#078) 11 Apr 2019 (#079) to 11	unfiltered & cooled	Conductivity meter (WTW Multilab 540), Alfred Wegener Institute in Potsdam, Germany (AWI)	±0.5 %

	Sept 2019 (#201)	unfiltered & frozen, thawed before analysis		
	13 Sept 2019 (#202) to 28 Aug 2020 (#362)			
	30 Aug 2020 (#363) to 23 Aug 2021 (#487)			
	26 Aug 2021 (#488) to 16 Aug 2022 (#612)	filtered & cooled	Conductivity meter (Milwaukee EC59 PRO), Lomonosov Moscow State University, Russia (MSU)	±2 %
Stable isotopes ($\delta^{18}O$, δD)	20 Apr 2018 (#001) to 13 Sept 2018 (#039)	unfiltered & cooled	Finnigan MAT Delta-S mass spectrometer, Alfred Wegener Institute in Potsdam, Germany (AWI)	δD: ±0.8 %, $\delta^{18}O$: ±0.1 %
	29 Sept 2018 (#043) to 6 Apr 2019 (#078)			
	11 Apr 2019 (#079) to 11 Sept 2019 (#201)			
	13 Sept 2019 (#202) to 28			

	Aug 2020 (#362)			
	30 Aug 2020 (#363) to 23 Aug 2021 (#487)			
	26 Aug 2021 (#488) to 02 Aug 2022 (#605)	unfiltered & cooled	PICARRO L2140i CRDS, Melnikov Permafrost Institute in Yakutsk, Russia (MPI)	δD: ±0.8 ‰, $\delta^{18}O$: ±0.1 ‰
Dissolved nutrients (Si, PO_4, NH_4, NO_2, NO_3)	20 Apr 2018 (#001) to 13 Sept 2019 (#39)	filtered & frozen	Continuous flow auto analyzer (San++, SKALAR) Otto Schmidt Laboratory in St. Petersburg, Russia (OSL)	N/A
	17 Sept 2018 (#040) to 11 Sept 2019 (#201)			
	13 Sept 2019 (#202) to 23 Aug 2021 (#487)	filtered & frozen	Continuous flow auto analyzer (AA3, SEAL Analytics) Helmholtz-Zentrum Hereon in Geesthacht, Germany (Hereon)	Detection limits: nitrate: 0.049µM, nitrite: 0.015µM ammonium: 0.092µM Silicate: 0.324µM phosphate: 0.011 µM
Total dissolved nitrogen and total dissolved phosphorus (TDN, TDP) &	20 Apr 2018 (#001) to 13 Sept 2018 (#039)	unfiltered & frozen	Persulfate oxidation and continuous flow auto analyzer (San++, SKALAR) Otto Schmidt Laboratory in St. Petersburg, Russia (OSL)	N/A

Total nitrogen and total phosphorus (TN, TP)	11 Sept 2019 (#201) to 28 Aug 2020 (#362), only TD/TN	filtered & frozen	Persulfate oxidation and continuous flow auto analyzer (AA3, SEAL Analytics) Helmholtz-Zentrum Hereon in Geesthacht, Germany (Hereon)	N/A
	26 Aug 2021 (#488) to 16 Aug 2022 (#612)	filtered & frozen	Persulfate oxidation, photometric (PE-5400UV spectrophotometer by ECROS LLC), Lomonosov Moscow State University in Moscow, Russia (MSU)	Standard error at p=0.05: TP/TDP: 0.0001+0.08*mg P/L TN/TDN: 0.04+0.077*mg N/L
DOC	20 Apr 2018 (#001) to 13 Sept 2018 (#039)	filtered & acidified & cooled	High temperature catalytic oxidation, TOC-VCPH (Shimadzu), Alfred Wegener Institute in Potsdam, Germany (AWI)	<5 % (against 8 standards of different concentrations)
	29 Sept 2018 (#043) to 6 Apr 2019 (#078)			
	11 Apr 2019 (#079) to 11 Sept 2019 (#201)			
	11 Sept 2019 (#201) to 2 May 2020 (#287)			
	9 May 2020 (#288) to 28			

	Aug 2020 (#362)			
	30 Aug 2020 (#363) to 23 Aug 2021 (#487)			
	26 Aug 2021 (#488) to 16 Aug 2022 (#612)	filtered & acidified & cooled	High temperature catalytic oxidation, TOPAZ NC, Informanalitika LLC, Lomonosov Moscow State University in Moscow, Russia (MSU)	<5 % (against 4 standards of different concentrations)
$a_{CDOM}(\lambda=200\text{-}800$ nm)	20 Apr 2018 (#001) to 13 Sept 2018 (#039)	filtered & cooled	Spectrophotometer, SPECORD 200 (Analytik Jena), Otto Schmidt Laboratory in St. Petersburg, Russia (OSL)	1 cm or 5 cm cuvette, spectral resolution: 1.6-1.8 nm
	29 Sept 2018 (#043) to 6 Apr 2019 (#078)	filtered & cooled	Spectrophotometer, LAMBDA 950 UV/Vis (PerkinElmer), German Research Centre for Geosciences in Potsdam, Germany (GFZ)	1 cm or 5 cm cuvette, spectral resolution: <0.05 nm
	11 Apr 2019 (#079) to 11 Sept 2019 (#201)	filtered & cooled	Spectrophotometer, SPECORD 200 (Analytik Jena), Otto Schmidt Laboratory in St. Petersburg, Russia (OSL)	1 cm or 5 cm cuvette, spectral resolution: 1.6-1.8 nm
	13 Sept 2019 (#202) to 23 Aug 2021 (#487)	filtered & cooled	Spectrophotometer, LAMBDA 950 UV/Vis (PerkinElmer), German Research Centre for	1 cm or 5 cm cuvette, spectral resolution: <0.05 nm

			Geosciencesin Potsdam, Germany (GFZ)	
	26 Aug 2021 (#488) to 16 Aug 2022 (#612)	filtered & cooled	Spectrophotometer, PE-5400-UV (ECROS LLC), Lomonosov Moscow State University in Moscow, Russia (MSU)	2 cm cuvette
FDOM	20 Apr 2018 (#001) to 13 Sept 2018 (#039)	filtered & cooled	Horiba AquaLog, Technical University of Denmark in Lyngby, Denmark (DTU)	1 cm cuvette
	29 Sept 2018 (#043) to 6 Apr 2019 (#078)			
	11 Apr 2019 (#079) to 11 Sept 2019 (#201)			
	13 Sept 2019 (#202) to 23 Aug 2021 (#487)			
DOC radiocarbon	30 Sept 2019 to 15 July 2021	frozen	EA-GIS-MICADAS, Alfred Wegener Institute in Bremerhaven, Germany (AWI)	2σ mean = 18 ‰
Ions (SO_4, Cl, Br, F, NO_3, PO_4)	20 Apr 2018 (#001) to 28	unfiltered & cooled, filtered before analysis	Ion chromatography, ICS 2100 (Thermo-Fischer), Alfred	Detection limits: F, Br = 0.05 mg L^{-1}, Cl, SO_4, NO_3 = 0.1 mg L^{-1}

	Mar 2019 (#077)		Wegener Institute in Potsdam, Germany (AWI)	
	6 Apr 2019 (#078) to 11 Sept 2019 (#201)	unfiltered & frozen, thawed & filtered before analysis		
	13 Sept 2019 (#202) to 2 May 2020 (#287)			
	9 May 2020 (#288) to 28 Aug 2020 (#362)			
	30 Aug 2020 (#363) to 23 Aug 2021 (#487)			
Ions (Cl, SO_4, F, NO_3)	26 Aug 2021 (#488) to 16 Aug 2022 (#612)	unfiltered & frozen, thawed & filtered before analysis	Ion chromatography, Concise ICSep An2, Lomonosov Moscow State University in Moscow, Russia (MSU)	N/A
Total dissolved elemental concentration (Al, Ba, Ca, Fe, K, Mg, Mn, Na, P, Si, Sr)	20 Apr 2018 (#001) to 28 Mar 2019 (#077)	unfiltered & cooled, filtered & acidified before analysis	Inductively coupled plasma optical emission spectroscopy, ICP-OES Optima 8300DV (Perkin Elmer), Alfred Wegener Institute in Potsdam, Germany (AWI)	Detection limits: Al, Ba, Fe, K, Na, Sr = 0.2 mg L^{-1}, Ca, Mg, Mn, P, Si = 0.1 mg L^{-1}
	6 Apr 2018 (#078) to 2 May 2020 (#287)	unfiltered & frozen, thawed & filtered &		

	9 May 2020 (#288) to 28 Aug 2020 (#362)	acidified before analysis		
Total dissolved elemental concentration (Na, K, Mg, Ca, Si, NH_4)	26 Aug 2021 (#488) to 16 Aug 2022 (#612)	unfiltered & frozen, thawed & filtered & acidified before analysis	Ion chromatography, Shodex IC YS-50, Lomonosov Moscow State University in Moscow, Russia (MSU)	N/A

3.1 River water temperature and electrical conductivity

For all sampling events (#001 to #612), the temperature of the river water was measured during sampling directly in the river at about 20 cm water depth using a handheld WTW COND 340I (accuracy ±0.5 %). The electrical conductivity (EC) of samples #079 to #487 (6 April 2019 to 23 August 2021) was measured on frozen samples that were thawed (24h at room temperature) after transport to the hydrochemistry laboratory at the AWI in Potsdam, Germany, using a WTW Multilab 540 conductivity meter (accuracy ±0.5 %). The EC of the first year (20 April 2018 to 6 April 2019; sample #001 to #078) were measured on unfrozen samples. Before each series of EC measurements, the conductivity meter was calibrated (cell constant was set for 25°C reference temperature) with a standard-solution with 1413 µS cm^{-1}. Between samples, the conductivity meter was cleaned with Milli-Q water and wiped dry. The EC for the last year (#488 to #611, 6 August 2021 to 14 August 2022) was measured on filtered samples (0.45 µm cellulose acetate) at the Lomonosov Moscow State University in Moscow (MSU) using a Milwaukee EC59 PRO conductivity meter (accuracy ±2 %). The river water temperature ranged between -0.3 and 20.2°C (Fig. 4b). During the ice-covered period, the river water temperature was very stable between -0.3 and 0.2°C. After ice break-up, the river water temperature increased from ~0°C to above 15°C within about two weeks. Between August and September, the river water temperature started to drop until reaching 0°C in mid-October.

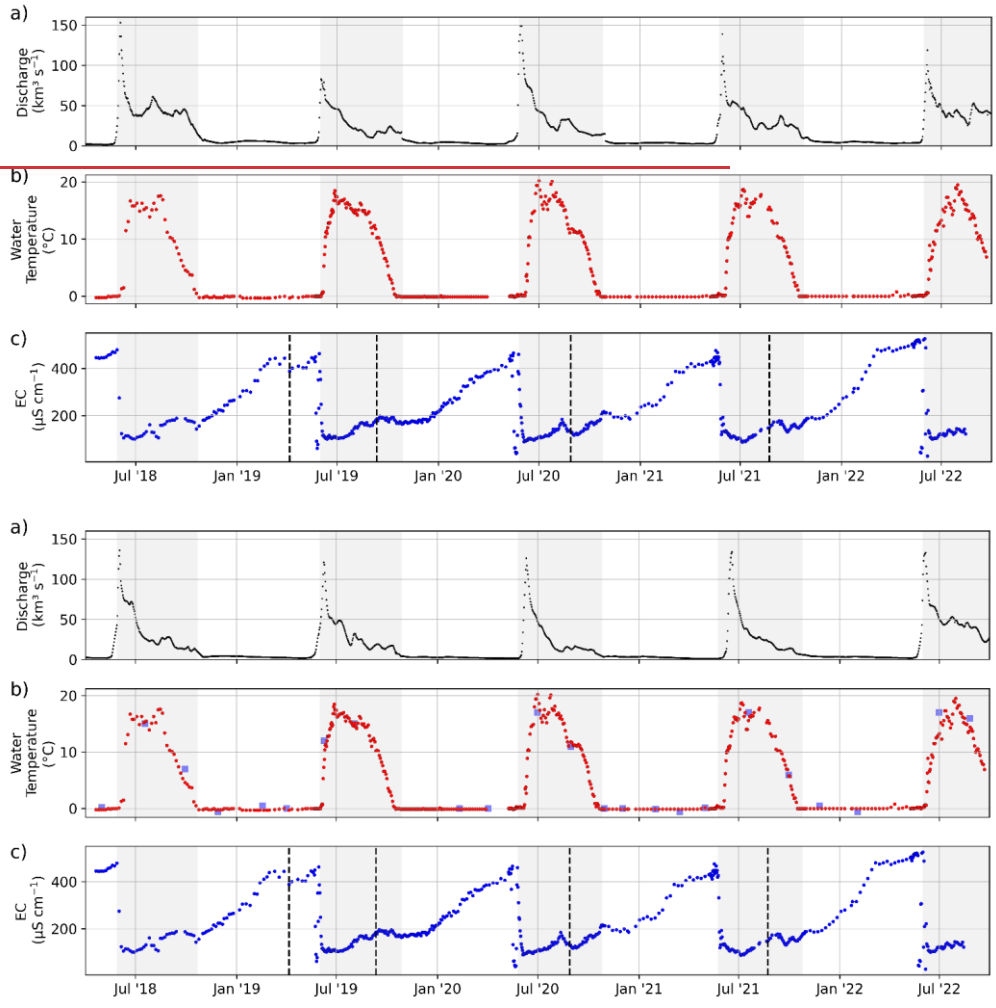

Figure 4: Time series of (a) discharge measured at Kyusyur and (b) river water temperature and (c) EC. Gray areas indicate the ice-free periods. Dashed black lines separate sample sets and indicate a change in measurement protocol and method (see Table 1). For comparison, we added temperature data sampled by the ArcticGRO program (blue squares in b).

The EC ranged between 29 and 526 µS cm^{-1} (Fig. 4c). Highest EC were observed at the end of the winter, right before ice break-up and the freshet of the river. In 2018, 2019, 2020, and 2022, the peak of the spring flood coincided with the lowest

annual EC. Only in 2021, the EC was lower in the first days of July compared to right after ice break-up in the beginning of June. In late winter 2022, EC was higher compared to previous years, whereas the lowest EC during the freshet was on a similar level as in previous years. EC was measured in five series (separated by dashed black lines in Fig. 4c). The data shows no offsets between those series. Note that a small number of samples exhibiting exceptionally low EC levels before the spring freshet could potentially be influenced by the pooling of meltwater from snow and ice during ice jamming events. For the samples #202 to #287 (13 September 2019 to 2 May 2020), we compared the EC from two sets of samples that were 1) frozen right after sampling and filtered only after transport and thaw before analysis, and 2) filtered right after sampling and transported unfrozen (cooled at +4°C) (Fig. B1).

3.2 Stable isotopes of water

Water samples for stable isotopes were filled immediately after sampling, untreated, into 10 mL HDPE vials, sealed tightly, and stored in the dark at 4°C. After transport, measurements for samples #001 to #487 (20 April 2018 to 23 August 2021) were conducted in five sample series (see Table 1) at the ISOLAB stable isotope facility at Alfred Wegener Institute in Potsdam (AWI) using a Finnigan MAT Delta-S mass spectrometer equipped with equilibration units for the online determination of hydrogen and oxygen isotopic composition. The measurement accuracy for hydrogen and oxygen isotopes was better than ±0.8 % and ±0.1 %, respectively (Meyer et al., 2000). Analysis for samples #488 to #605 (26 August 2021 to 2 August 2022) were conducted at the Melnikov Permafrost Institute in Yakutsk (MPI) using a PICARRO L2140i Isotopic Water Liquid Analyzer for the online determination of the hydrogen and oxygen isotopic composition in water samples using Cavity Ring-Down Spectroscopy (CRDS). PICARRO L2130i CRDS uses a laser with an effective path length of up to 20 kilometers to quantify spectral features of gas phase molecules by scanning repeatedly the absorption lines of $H_2{}^{16}O$, $H_2{}^{18}O$, and $HD^{16}O$ in a temperature and pressure controlled optical cavity. The PICARRO L2140i Isotopic Water Liquid Analyzer simultaneously measures isotopic ratios of D/H and $^{18}O/^{16}O$ in liquid water providing both, $\delta^{18}O$ and δD data from one aliquot. Samples from 2 mL glass vials are automatically injected into a temperature controlled and stabilized Vaporizer Unit (A0211) held at high temperature with the vapor sent to the analyzer. At least three standards are used for quality control, selected according to the expected isotopic composition of the samples. For a single CRDS stable isotope measurement, about 2 µL of water is injected. This process is repeated six times resulting in both, final dD and $d^{18}O$ values (which refers to the permille difference related to V-SMOW). These values are corrected for drift and memory effects. The precision of long-term standard measurements for the H and O isotope composition is better than ±0.8 ‰ and ±0.10 ‰, respectively. The data are reported as δD and $\delta^{18}O$ values, which is the per mille (‰) difference from standard V-SMOW. The deuterium excess (d-excess) is calculated by

$$d - excess = \delta D - 8 * \delta 18O, \quad (1)$$

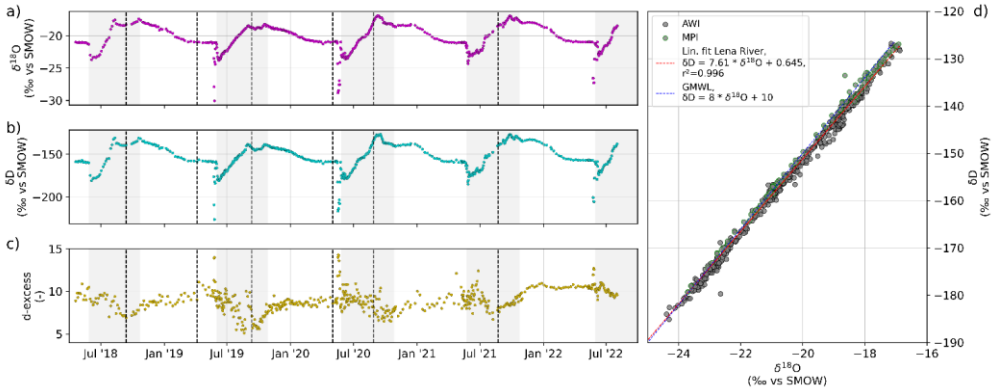

505 **Figure 5: Time series of (a) $\delta^{18}O$, (b) δD, and (c) d-excess. The scatterplot in (d) shows the relationship between $\delta^{18}O$ and δD of the Lena River, where samples measured at the Alfred Wegener Institute are indicated by a black outline and samples measured at the Melnikov Permafrost Institute by a green outline. The linear regression is shown by the solid red line and the dashed blue line shows the global meteoric water line after Craig (1961).**

Both, δD and $\delta^{18}O$ were at their lowest during the beginning of the ice-free season and increased over its course. Late summer
510 and early fall variability due to rainfall events precedes the formation of ice. Once the ice cover started to form, the isotope signature decreased gradually over the fall and winter until dilution with snow melt at break-up restarted the annual cycle. Similar as for EC, a small number of samples during initial breakup had much lower values (< -25 ‰ $\delta^{18}O$ and < -180 ‰ δD) and might be influenced by the pooling of meltwater from snow and ice during ice jamming events. The stable isotopes shown in Fig. 5 have been measured in seven sets (separated by dashed vertical lines) and in two different labs (see Table 1). There
515 are no apparent offsets between sample sets. The d-excess of the sample set that was measured at the MPI (#488 to #612) shows less noise compared to previous sets.

3.3 Dissolved organic carbon concentrations and absorption of colored dissolved organic matter

For dissolved organic carbon (DOC), the sample water was filtered right after sampling through a 0.45 µm cellulose acetate filter, which had been pre-rinsed with 20 mL of sample. DOC samples were filled into a pre-rinsed 20 mL glass vial and
520 acidified with 25 µL HCl Suprapur (10 M) and stored in the dark at 4°C. After transport, DOC samples #001 to #487 were analyzed at the hydrochemistry laboratory at AWI Potsdam. DOC concentrations were analyzed using high temperature catalytic oxidation (TOC-V_{CPH}, Shimadzu). Three replicate measurements of each sample were averaged. After every ten samples, a blank (Milli-Q water) and a standard was measured. Eight different commercially available certified standards covered a range between 0.49 mg/L (DWNSVW-15) and 100 mg/L (Std. US-QC). The results of standards provided an
525 accuracy no worse than ± 5 %. DOC concentrations for samples #488 to #612 (26 August 2021 to 16 August 2022) were analyzed at Lomonosov Moscow State University (MSU) using a TOPAZ NC, Informanalitika LLC (Russia). Three replicate

measurements of each sample were averaged and three standards (5, 15, and 100 mg L^{-1}) as well as blanks (Milli-Q water) were used to ensure high accuracy of the measurements. For the period 10 September 2021 to 31 July 2022, total carbon and inorganic carbon concentrations were measured on unfiltered samples (Fig. C2). For the absorption of colored dissolved organic matter ($a_{CDOM}(\lambda)$), the samples were filtered right after sampling through a 0.45 µm cellulose acetate filter, which had been rinsed with 20 mL sample water. $a_{CDOM}(\lambda)$ samples were collected into pre-rinsed 50 mL amber glass bottles that were stored in the dark at 4°C until analysis. After transport, $a_{CDOM}(\lambda)$ for samples #001 to #039 (20 April 2018 to 13 September 2018) and #079 to #201 (11 April 2019 to 11 September 2019) were measured at the Otto Schmidt Laboratory for Polar and Marine Research (OSL) in Saint Petersburg, Russia, using a double beam SPECORD 200 (Analytik Jena) spectrophotometer. Samples #043 to #078 (29 September 2018 to 06 April 2019) and #202 to #478 (13 September 2019 to 23 August 2021) were measured at the German Research Center for Geosciences (GFZ) in Potsdam, Germany using a double beam LAMBDA 950 UV/Vis (PerkinElmer) spectrophotometer. Samples #488 to #612 (26 August 2021 to 16 August 2022) were measured at MSU, Russia using a PE-5400-UV (ECROS LLC) spectrophotometer. The absorbance (A) was measured between 200 and 800 nm in 1 nm steps using a 1, 2, or 5 cm cuvette, depending on the expected concentration of dissolved organic matter. Napierian absorption (a) was calculated from the resulting absorbance measurements via

$$aCDOM(\lambda) = \frac{2.303 * A(\lambda)}{l}, \quad (2)$$

where l is the path length (length of cuvette in meter). Every five to ten samples, the reference sample (Milli-Q water) was exchanged and a blank was measured to avoid artifacts from instrument drift.

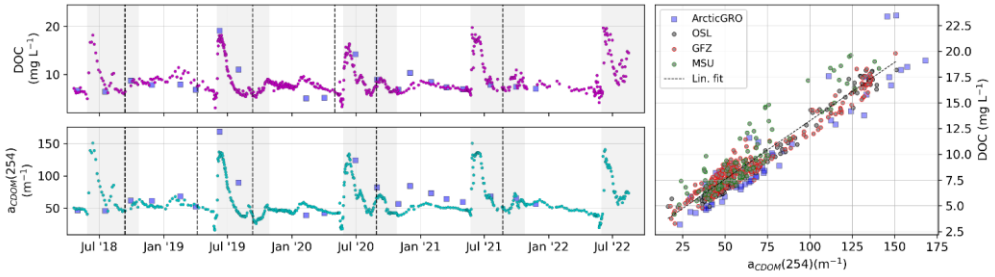

Figure 6: Time series of (a) DOC and (b) $a_{CDOM}(254)$. Dashed black lines separate sample sets and indicate a possible change in measurement protocol and method (see Table 1). (c) Relationship between $a_{CDOM}(254)$ and DOC where the dashed black line shows the linear fit of all data. The outline colour of the circles indicates the lab where samples were measured. For comparison, we show data sampled by the ArcticGRO program (blue squares).

The DOC concentration ranged between 3.1 and 19.8 mg L^{-1} (Fig. 6a). $a_{CDOM}(254)$ ranged between 16.4 and 150.9 m^{-1} (Fig. 6b). Low DOC concentrations and $a_{CDOM}(254)$ occurred either in the late winter, or in summer during periods of low discharge. The highest annual DOC and $a_{CDOM}(254)$ occurred during the spring freshet, when discharge was the highest. $a_{CDOM}(254)$ and DOC showed a very strong linear relationship (r^2=0.92). The samples measured at MSU showed a significantly lower r^2 (=0.85), compared to the samples measured at GFZ (r^2=95) or OSL (r^2=0.98). Note that while we only show a_{CDOM} at the

wavelength 254 nm, the dataset in Juhls et al. (2020b) contains all wavelengths between 200 and 800 nm. DOC and $a_{CDOM}(254)$ generally agrees with data from ArcticGRO sampled several hundrets of km further upstream, however shows a generally lower DOC to $a_{CDOM}(254)$ ratio compared to our data. Based on DOC and $a_{CDOM}(\lambda)$, we calculated three optical indices as indicators for the chemical composition and molecular structure of the organic matter: Specific Ultraviolet Absorbance at 254 nm ($SUVA_{254}$), the spectral slopes of $a_{CDOM}(\lambda)$ between 275 and 295 nm (S275-295), and the slope ratio (SR). These three indices are reported to correlate with the aromaticity and molecular weight of bulk DOC (Helms et al., 2008; Weishaar et al., 2003). The change in S275-295 has been reported to be a good indicator for photodegradation of DOM (Fichot et al., 2013; Fichot and Benner, 2012; Helms et al., 2008). $SUVA_{254}$ (m^2 g C^{-1}) was calculated by dividing the decadal absorption A/l (m^{-1}) at 254 nm by DOC concentration (mg L^{-1}). The $SUVA_{254}$ ranged between 1.41 and 3.89 mg L^{-1} with highest values after the freshet and lowest values during winter and low discharge periods in summer. S275–295 was determined by fitting the data for the wavelength ranges 275–295 nm to the exponential function (Helms et al., 2008):

$$aCDOM(\lambda) = aCDOM(\lambda 0) * e^{-S(\lambda - \lambda 0)}, \quad (3)$$

where $a_{CDOM}(\lambda_0)$ is the absorption coefficient at reference wavelength λ_0 and S is the spectral slope of $a_{CDOM}(\lambda)$ for the chosen wavelength range. S275-295 ranged between 0.0130 and 0.0182 nm^{-1}. The SR was calculated by dividing the spectral slope from 275 to 295 nm by the spectral slope between 350 and 400 nm. SR ranged between 0.814 and 1.36, not including the last set of samples (from 26 August 2021). This set, measured with the PE-5400-UV spectrophotometer at the MSU, shows noisy results for longer wavelengths visible in the S350-400 that is used to calculate SR. Consequently, SR data for that sample series is not recommended to be used. The results for S275-295 of this sample series, however, are comparable with previous sample series.

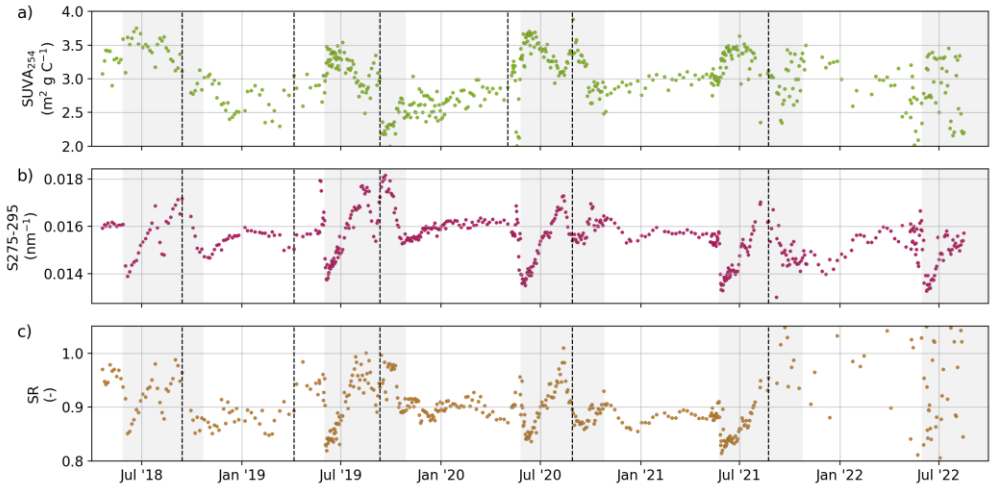

Figure 7: (a) Time series of $SUVA_{254}$, (b) S275-295 and (c) SR. Dashed black lines separate sample sets and indicate a possible change in measurement protocol and method (see Table 1)

3.4 Fluorescent dissolved organic matter

Fluorescence measurements were carried out at the Technical University of Denmark on a Horiba Aqualog with a 1 cm quartz cuvette (Suprasil grade, Helma GmbH) using the same sample as for $a_{CDOM}(\lambda)$. Fluorescence emission was recorded between 220 and 620 nm (increment ~3.3 nm) at excitation wavelengths between 240 nm and 600 nm (increment 3 nm). The accuracy of the optical components and the immaculacy of cuvettes were validated daily (Wünsch et al., 2015). Fluorescence excitation-emission matrix (EEM) data were processed in Matlab (MathWorks Inc.) using the drEEM toolbox (v0.6.3, Murphy et al. (2013). Inner filter effects were compensated using the absorbance-based method (Kothawala et al., 2013) and the fluorescence counts were converted into Raman units (R.U.) using the water blank's (sealed reference cuvette) Raman emission band at 350 nm. Raman and Rayleigh scatter were removed from each EEM without interpolation.

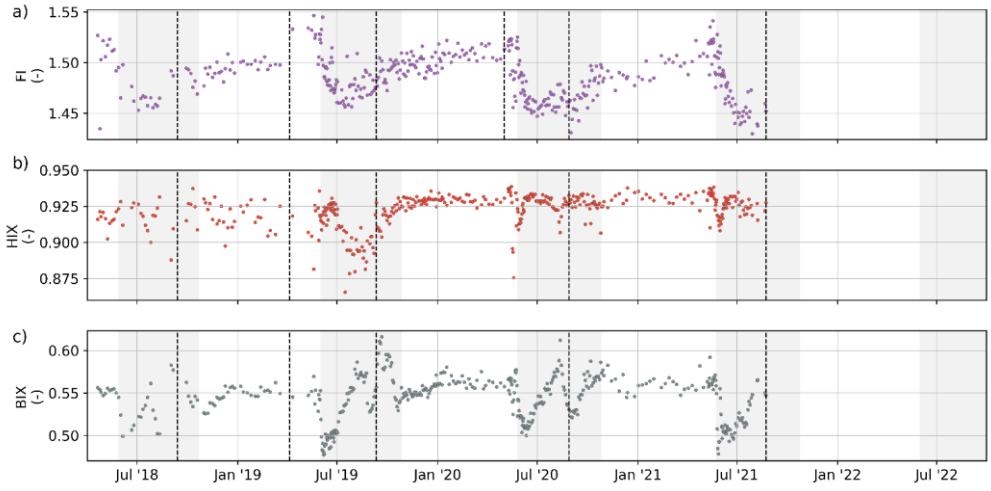

Figure 8: (a) Time series of Fluorescence Index (FI), (b) Humification Index (HIX) and (c) Biological Index (BIX). Dashed black lines separate sample sets and indicate a possible change in measurement protocol and method (see Table 1).

Fluorescence-derived DOM optical indices are proxies for the character of DOM with respect to its degree of humification and biological degradation, therefore giving insights into DOM's source (Fig. 8). The Fluorescence Index (FI) was determined as the ratio between the emission intensities at 470/520 nm for an excitation wavelength of 370 nm (Maie et al., 2006). FI values generally ranged between 1.2 and 2, indicating terrestrial or microbial origin of DOM, respectively (D'Andrilli et al., 2022; McKnight et al., 2001). The FI values for our samples ranged between 1.43 and 1.54 (median 1.48), with the highest values observed just before the ice-free period, decreasing drastically after the ice breaks up. The Humification Index (HIX) estimates

the degree of humification of DOM (Zsolnay, 2003; Zsolnay et al., 1999). We calculated it as modified by Ohno (2002) as the ratio of the areas of two spectral wavelength regions in the emission spectra for an excitation at 254 nm and obtained it as:

$$HIX = \frac{H}{(H+L)}, \quad (4)$$

where H is the area between 435 and 480 nm in the emission spectra and L is the area in the emission spectra between 300 and 345 nm. An increase in the degree of aromaticity (humification) will be associated with higher HIX values. HIX values ranged from 0.78 to 0.93 (median 0.92) showing relatively steady values during the ice-covered season with values decreasing at the beginning of the ice-free season. The biological index (BIX) is a proxy used to assess the biological modification of DOM. The BIX is obtained by calculating the ratio of the emission at 380 and 430 nm, excited at 310 nm (Huguet et al., 2009):

$$BIX = \frac{IEm380}{IEm430}. \quad (5)$$

High BIX values correspond to autochthonous origin of DOM, i.e., freshly released DOM, whereas low BIX values indicate allochthonous DOM (Huguet et al., 2009). BIX values varied between 0.48 and 0.61 (median 0.54) during the sampling period. Values presented low variability during the ice-covered periods, followed by a rapid decrease at the beginning of the ice-free season, then rapidly increasing and reaching the highest values. The underlying fluorescence phenomena were distinguished using parallel factor analysis (PARAFAC) with the N-way toolbox algorithms (Andersson and Bro, 2000). Prior to modeling, excitation scans shorter than 250 and longer than 450 nm and emission scans shorter than 312 and longer than 600 nm were deleted to save computation time. EEMs were normalized by division with the 1.2th root of their standard deviation to give samples with different overall fluorescence a similar leverage. Models with two to eight components were explored. All models were constrained to fit components with positive scores and loadings (i.e. nonnegativity). Models were initialized with random numbers and the best model (with the lowest model error) out of 50 solutions was selected. A maximum of 2500 iterations was allowed and relative change in fit of 10^{-6} was chosen as the convergence criterion. Ultimately, the seven-component model was chosen as the most appropriate approximation and its loadings were validated using the split-half approach. Seven fluorescent DOM components (Fmax) were isolated with PARAFAC (Fig. 9a). Overall, all components presented the same temporal patterns with relatively steady values during the ice-covered season, followed by a decrease just before the ice break-up and rapidly increasing and quickly reaching the highest values shortly after ice break-up (Fig. 9b). Components 1 and 2 (C1 and C2, respectively) showed fluorescence peaks in the UV range, which are generally associated with autochthonous DOM such as protein-like compounds (Coble, 2007). The fluorescence intensities of C1 and C2 varied from 0.04 to 0.54 R.U. and from 0.03 to 0.3 R.U., respectively. C3 to C7 showed a fluorescence peak in the visible wavelength range (>400 nm), which is generally associated with terrestrial humic-like compounds (Coble, 2007). C3 and C4 showed the highest fluorescence intensities, varying from 0.18 to 1.38 R.U. and from to 0.08 R.U. to 2.03 R.U., respectively. C5 and C6, ranged from 0.30 to 2.8 R.U. and from 0.06 to 0.62 R.U., respectively, whereas C7 values ranged between 0.12 and 1.05 R.U..

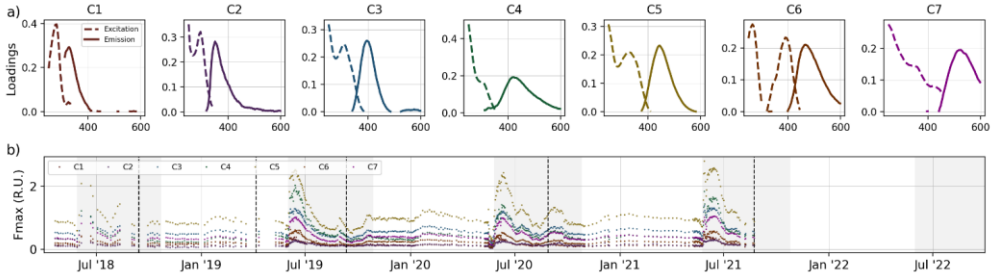

Figure 9: (a) Loading excitation and emission spectra of the seven identified PARAFAC components. (b) Time series of the Fmax loadings for the seven components. Dashed black lines separate sample sets.

3.5 DOC radiocarbon

Samples for DOC $\Delta^{14}C$ analysis were taken biweekly from 30 September 2019 to 15 July 2021. For each sample, an acid-washed 250 mL HDPE bottle was rinsed two times with river water before filling it with the sample in order to preempt contamination from sources such as outboard motor exhaust or dust particles. Water was collected upstream from the boat and operator to ensure the utmost integrity of the samples. After sample collection, each bottle was promptly sealed and kept frozen at a temperature of -20°C during subsequent transportation and storage. Radiocarbon contents of DOC were analyzed using a MIniature CArbon DAting System (MICADAS) at Alfred Wegener Institute in Bremerhaven, Germany and methods described in Mollenhauer et al. (2021). In the laboratory, water samples were thawed and filtered over 0.75 µm glass fiber filters (GF/F, Whatman). Dissolved organic matter (DOM) was concentrated by evaporation of water using a rotary evaporator. Concentrated DOM was transferred into silver liquid cups (70 µL, Elementar part#: 200010387) and dried completely on a hot plate followed by storage in a dessicator kept at 40°C. After drying, silver cups were folded into small packages and combusted in an elemental analyzer (EA, Elementar varioIsotope), coupled to the Ionplus Gas Interface System (GIS; Wacker et al. (2013), allowing the transfer of CO_2 directly into the hybrid ion source of the MICADAS. Samples were analyzed as gas for a 12-minute measurement cycle, data were evaluated using the BATS software package (Wacker et al., 2013) and normalized against Oxalic Acid II standard gas (CO_2 produced from Oxalic Acid II, NIST SRM4990C) and blank corrected against ^{14}C-free CO_2. Secondary blank correction was performed using process blank determination according to the method of Sun et al. (2020), and errors were propagated following Wacker and Christl (2011). Results are reported as ^{14}C, conventional radiocarbon ages (years BP) (Stuiver and Polach, 1977).

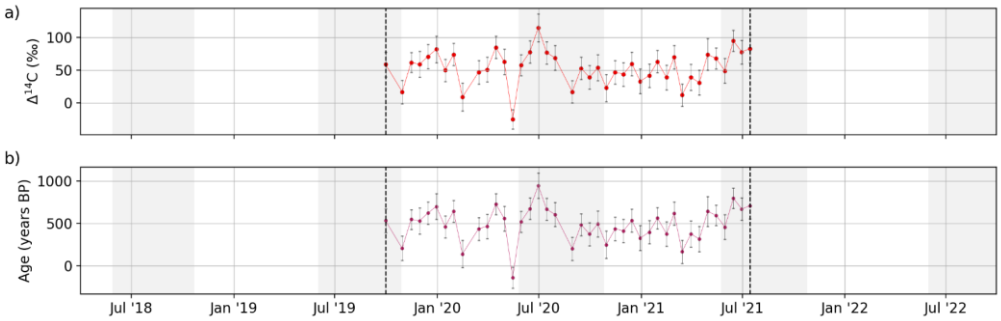

Figure 10: (a) $\Delta^{14}C$ of DOC and the 2 x standard deviation (2σ) shown as error bars, (b) corresponding age and the 2 x standard deviation (2σ) shown as error bars. Dashed black lines indicate the start and end date of the set of samples that were analyzed.

No clear seasonal patterns were identified in the radiocarbon contents of DOC, with $\Delta^{14}C$ values ranging between -25 ‰ and 115 ‰ (Fig. 10a) and corresponding conventional radiocarbon ages between -945 and 138 years (Fig. 10b). The lack of clear seasonal differences may be due to the lower number of samples and the reduced sampling period.

3.6 Nutrients

Samples for dissolved inorganic nutrient (ammonium (NH_4), nitrite (NO_2), nitrate (NO_3), phosphate (PO_4), and silicate (Si)) analysis as well as for total dissolved nitrogen and total dissolved phosphorus (TDN, TDP) were filtered through a 0.45 µm cellulose acetate filter, which had been rinsed with 20 mL sample water. Nutrients/TDN/TDP samples were filled into pre-rinsed 20 mL PE bottles and stored frozen at -18°C until measured. For TN/TP (total nitrogen and total phosphorus), unfiltered samples were filled into pre-rinsed 20 mL PE bottles and stored frozen at -20 °C until measured. TN/TDN and TP/TDP for samples #001 to #039 (20 April 2018 to 13 September 2018) and dissolved inorganic nutrients for samples #001 to #201 (20 April 2018 to 11 September 2019) were measured at the Otto Schmidt Laboratory in St. Petersburg, Russia. Dissolved inorganic nutrients were analyzed on an automated continuous flow system (San++, SKALAR, Netherlands) with standard colorimetric techniques (Aminot et al., 2009). For the determination of TN/TDN and TP/TDP, the persulfate oxidation method (Knapp et al., 2005) was used. The first step was the oxidation of total dissolved nitrogen (TDN, the sum of nitrate, nitrite, ammonium and dissolved organic nitrogen (DON)) to nitrate and TDP to phosphate. Therefore, 24 ml of the sample plus 2 ml of persulfate oxidizing reagent (POR) was added to a Teflon bottle. The POR contained ACS-grade sodium hydroxide, certified ACS-grade boric acid and certified ACS-grade potassium persulfate, which was recrystallized three times (Hansen and Koroleff, 2007). The digestion was performed by autoclaving at 121°C. In the same digestion also the total phosphorus was measured. Reagent blank was below 0.1 µM. Environmental matrix reference materials (Environment and Climate Change Canada) were used as tracking standards in every batch of samples. TN and TP for samples from #201 to #362 and dissolved inorganic nutrients for samples #202 to #487 were measured at the Helmholtz-Zentrum Hereon in Geesthacht, Germany.

Nutrient concentrations were analyzed in duplicates using an automated continuous flow system (AA3, Seal Analytical, Germany) and standard colorimetric techniques (Hansen and Koroleff, 2007). Detection limits were 1 μM for nitrate and silicate, 0.5 μM for nitrite, ammonium and phosphate. For the determination of TDN/TDP, we used the same method as described above for the previous samples. For digestion, a microwave (CEM, Mars 5) was used. The reagent blank was always <2 μM. As reference, internal standards of ammonium sulfate and urea were used. In the same digestion, total phosphorus was measured. Reagent blank was below 0.1 μM. For the analysis of TDN and TNP, we used the same method as was used for unfiltered water samples (total). The results of standards provided an accuracy better than ± 10 %. TN/TDN, TP/TDP for samples #488 to #612 were measured at the MSU using a PE-5400UV spectrophotometer by ECROS LLC (Russia). Frozen samples were thawed at room temperature in bulks of 10 to 20 samples at once and processed the same day as soon as they reached the appropriate temperature. Concentrations of inorganic phosphorus (orthophosphate) in filtered and unfiltered samples were determined photometrically by the Murphy-Riley method (molybdenum blue reaction of orthophosphate with ammonium molybdate and antimony potassium tartrate in sulphuric acid, reduced by ascorbic acid, measured at wavelength 885 nm in a 5 cm cuvette). Approved detection range of the specific method used was 0.005-0.100 mg/L of orthophosphate (or 0.0016-0.033 mg P/L), standard error at p=0.05 was 0.0001+0.08*X, where X is the determined concentration in mg P/L. To account for turbidity, two measurements of optical density were made: 1) without ascorbic acid, 2) with ascorbic acid. Total phosphorus concentrations were determined after persulphate digestion (samples heated in an autoclave at 121°C for 1 hour with ammonium persulphate added) by the same method as for inorganic phosphorus. TN concentrations were determined by alkaline persulphate digestion (samples autoclaved at 120°C for 90 minutes with potassium persulphate and sodium hydroxide, then measured in a 1 cm quartz cuvette at 207 nm wavelength after adding sulphuric acid). Approved detection range of the specific method used was 0.1-6.0 mg N/L, standard error at p=0.05 is 0.04+0.077*X, where X is the determined concentration in mg N/L. Calibration coefficients for the spectrophotometer were obtained by running the described procedures on solutions diluted from a standard 0.5 g/L solution of phosphate ion and 0.5 g/L solution of TN.

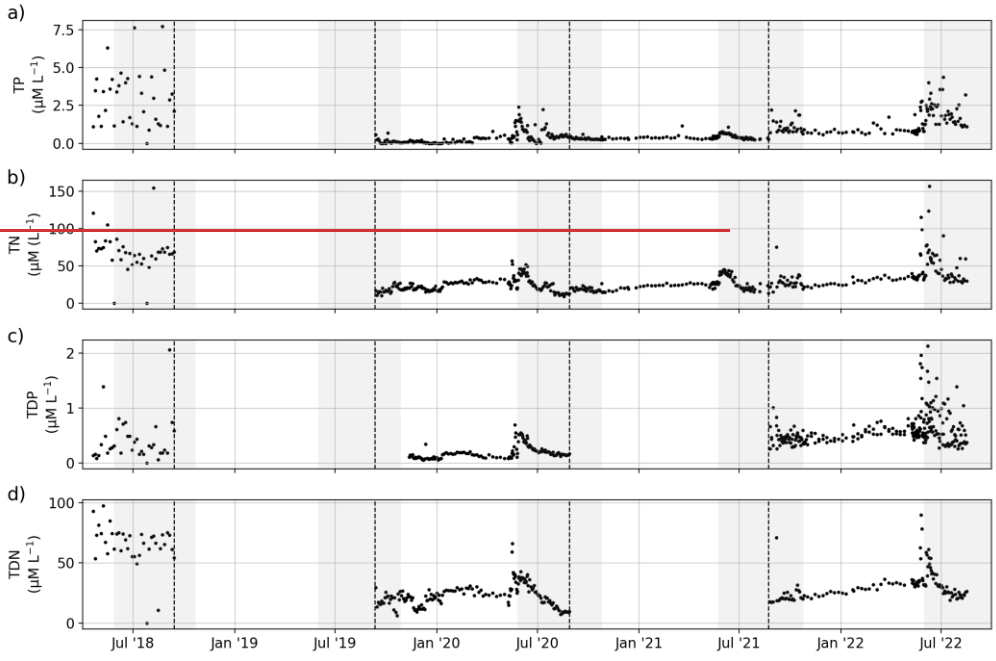
a)
TP
(µM L⁻¹)
7.5
5.0
2.5
0.0
b)
TN
(µM (L⁻¹)
150
100
50
0
c)
TDP
(µM L⁻¹)
2
1
0
d)
TDN
(µM L⁻¹)
100
50
0
Jul '18
Jan '19
Jul '19
Jan '20
Jul '20
Jan '21
Jul '21
Jan '22
Jul '22

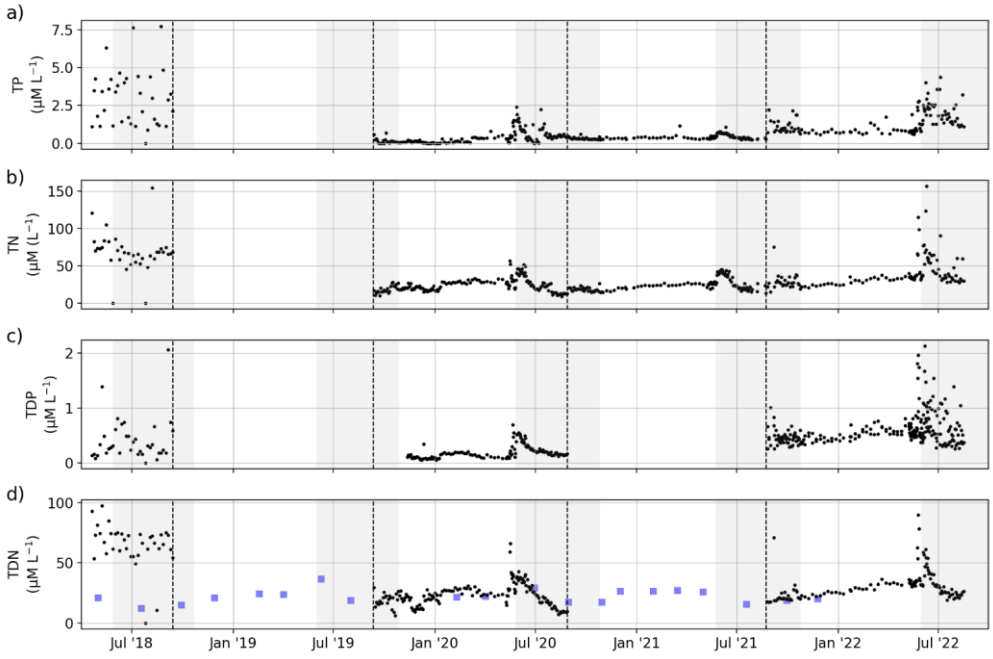

Figure 11: Concentrations of (a) total phosphorus, (b) total nitrogen, (c) total dissolved phosphorus, and (d) total dissolved nitrogen. Dashed black lines separate sample sets and indicate a possible change in measurement protocol and method (see Table 1). For comparison, we added data sampled by the ArcticGRO program (blue squares).

TN/TDN, TP/TDP showed peaks during the freshet in June and decreasing concentrations throughout the summer. The difference in noisiness of the data between the four available sample sets indicate varying quality of the analysis.

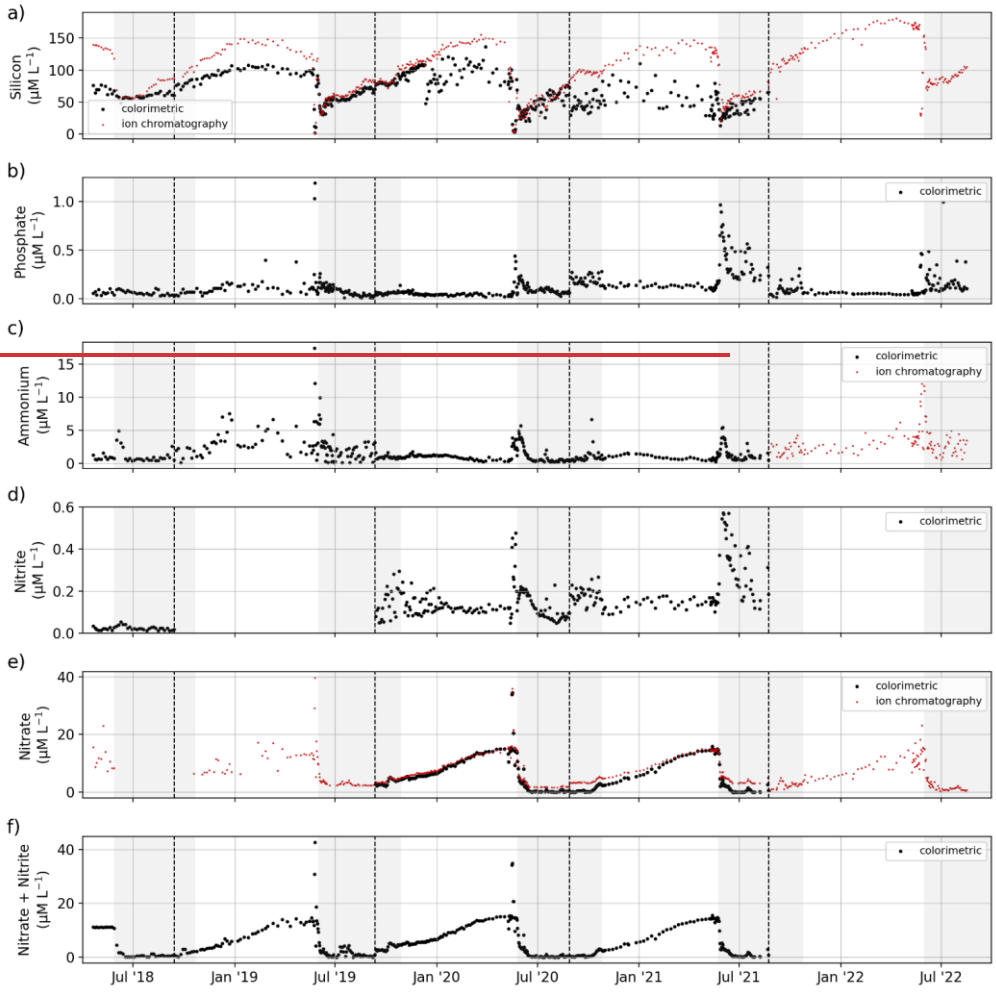
a)
Silicon (µM L⁻¹)
colorimetric
ion chromatography
b)
Phosphate (µM L⁻¹)
colorimetric
c)
Ammonium (µM L⁻¹)
colorimetric
ion chromatography
d)
Nitrite (µM L⁻¹)
colorimetric
e)
Nitrate (µM L⁻¹)
colorimetric
ion chromatography
f)
Nitrate + Nitrite (µM L⁻¹)
colorimetric
Jul '18
Jan '19
Jul '19
Jan '20
Jul '20
Jan '21
Jul '21
Jan '22
Jul '22

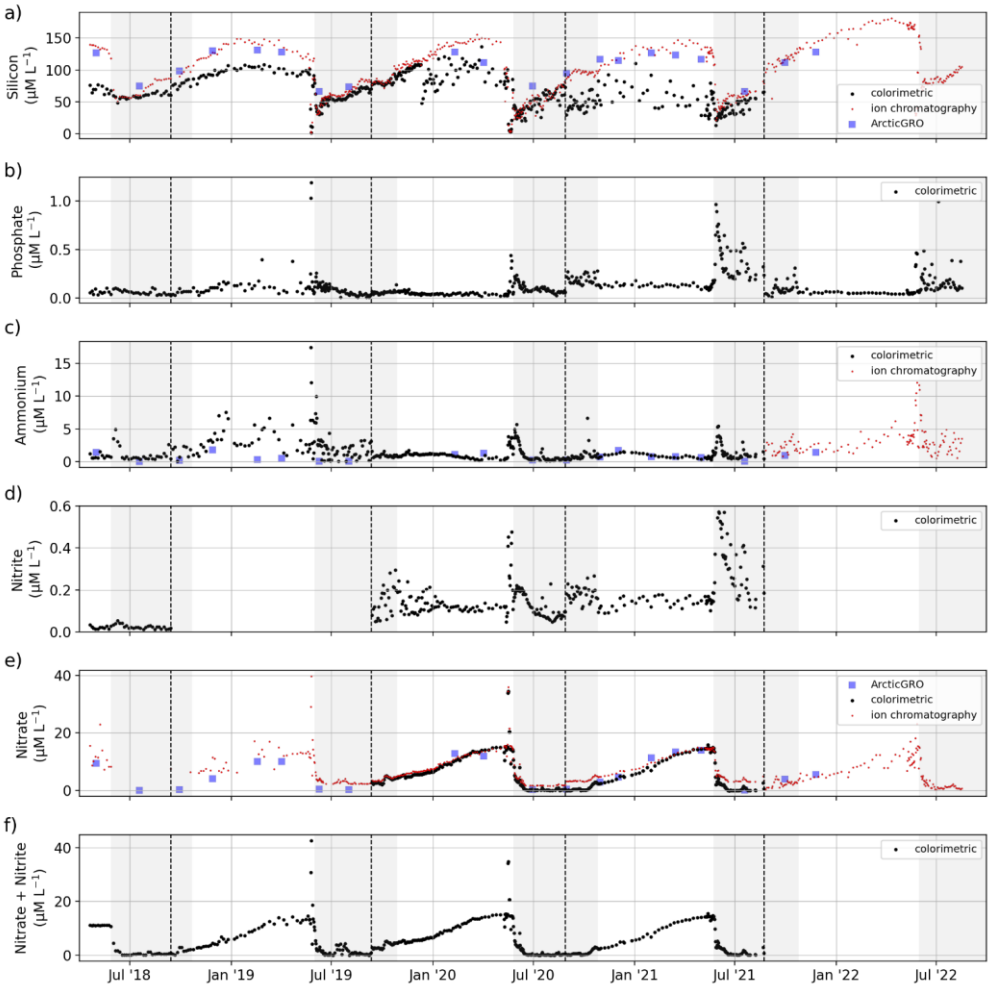

Figure 12: Concentrations of dissolved inorganic nutrients: (a) Si, (b) PO_4, (c) NH_4, (d) NO_2, (e) NO_3, (f) NO_2+NO_3 determined by colorimetric/photometric methods (black) and by ion chromatography (red). Dashed black lines separate sample sets and indicate a possible change in measurement protocol and method (see Table 1). For comparison, we added data sampled by the ArcticGRO program (blue squares).

PO_4, NH_4 and NO_2 showed annual peak concentrations during the freshet in June whereas NO_3 showed a gradual increase during the winter and a sudden decrease during the freshet. Si concentrations increased from the freshet until mid/end-winter. Comparing TDN, Si, NH_4, and NO_3 with data from ArcticGRO reveals a good agreement between the datasets.

Formatted: Subscript

Formatted: Subscript

3.7 Dissolved elemental and ion concentrations

Samples #079 to #487 (6 April 2019 to 23 August 2021) analyzed for concentrations of major dissolved elements and ions were frozen untreated directly after sampling. After transport, samples were thawed (24h at room temperature) in the hydrochemistry laboratory at the hydrochemistry laboratory at AWI in Potsdam, Germany. They were then filtered using a syringe-mounted 0.45 µm cellulose acetate filter and kept cool and dark until analysis. Samples for the first year (20 April 2018 to 6 April 2019; sample #001 to #078) were filtered right after sampling and transported cool and dark. Samples #079 to #487 were frozen right after sampling and thawed and filtered after transport prior to analysis. Concentrations of major ions (Sulfate (SO_4), bromide (Br), nitrate (NO_3), phosphate (PO_4), chloride (Cl), and fluoride (F)) were determined using ion chromatography (Thermo-Fischer ICS 2100; Weiss, (2001)). A blank (Milli-Q water) and a standard were measured every ten samples. A commercially available certified standard in two different dilutions (1:5 and 1:10) was used to determine measurement accuracy and the detection limits (Table 1). Total dissolved elemental concentration (aluminum (Al), barium (Ba), calcium (Ca), iron (Fe), potassium (K), magnesium (Mg), manganese (Mn), sodium (Na), phosphorus (P), silicon (Si), and strontium (Sr)) samples #001 to #078 were filtered right after sampling and cooled. Samples #079 to #487 were frozen right after sampling and thawed after transport and filtered prior to analysis. Then, samples were acidified with 65 % HNO3 (65 % suprapur) and were measured with inductively coupled plasma optical emission spectroscopy (ICP-OES; Perkin Elmer Optima 8300DV; Boss and Fredeen, (1997)). For the samples #202 to #287 (13 September 2019 to 2 May 2020), we compared elemental and ion concentrations from two sets of samples that were 1) frozen right after sampling and thawed and filtered only after transport, and 2) filtered right after sampling and transported unfrozen (cooled at +4°C). Comparing the results of the two sets shows that differences in sample processing affect elemental and ion concentrations in ways that introduce systematic biases (Fig. B2 & B3). These biases differ in magnitude and direction depending on parameter, but for most parameters freezing results in lower concentrations. Samples #488 to #612 (26 August 2019 to 16 August 2021) were treated identically to the samples #079 to #487, but measured at the MSU. Concentrations of major dissolved elements and ions were measured using ion chromatography using a Concise ICSep An2 column for major ions (Cl, SO_4, F, NO_3) and a Shodex IC YS-50 column for total dissolved elemental concentration (Na, K, Mg, Ca, Si, NH_4). Most dissolved elemental and ion concentrations (SO_4, NO_3, Ba, Cl, F, Ca, K, Mg, Na, Si, Sr) increased during the winter (similar to EC, Fig. 4) and decreased sharply during the freshet (Fig. 13 & 14). Fe and Mn showed a strong peak and their annual maximum during the freshet. Al and P did not indicate clear seasonal patterns. The different protocol (transport of samples cooled vs transport of samples frozen) between samples <#077 and >#077 resulted in visible offsets between the sample sets (i.e., F, Al, Mn, ..). The differences between unfrozen and frozen samples across different sample sets seem similar to those shown in Appendix B (comparing frozen and unfrozen samples of the same sample set).

In addition, we compared some of the dissolved elemental and ion concentrations with those measured by the ArcticGRO program, which shows a generally good agreement. Some stronger differences might be related to the earlier arrival of changing seasons at the ArcticGRO sampling location further south.

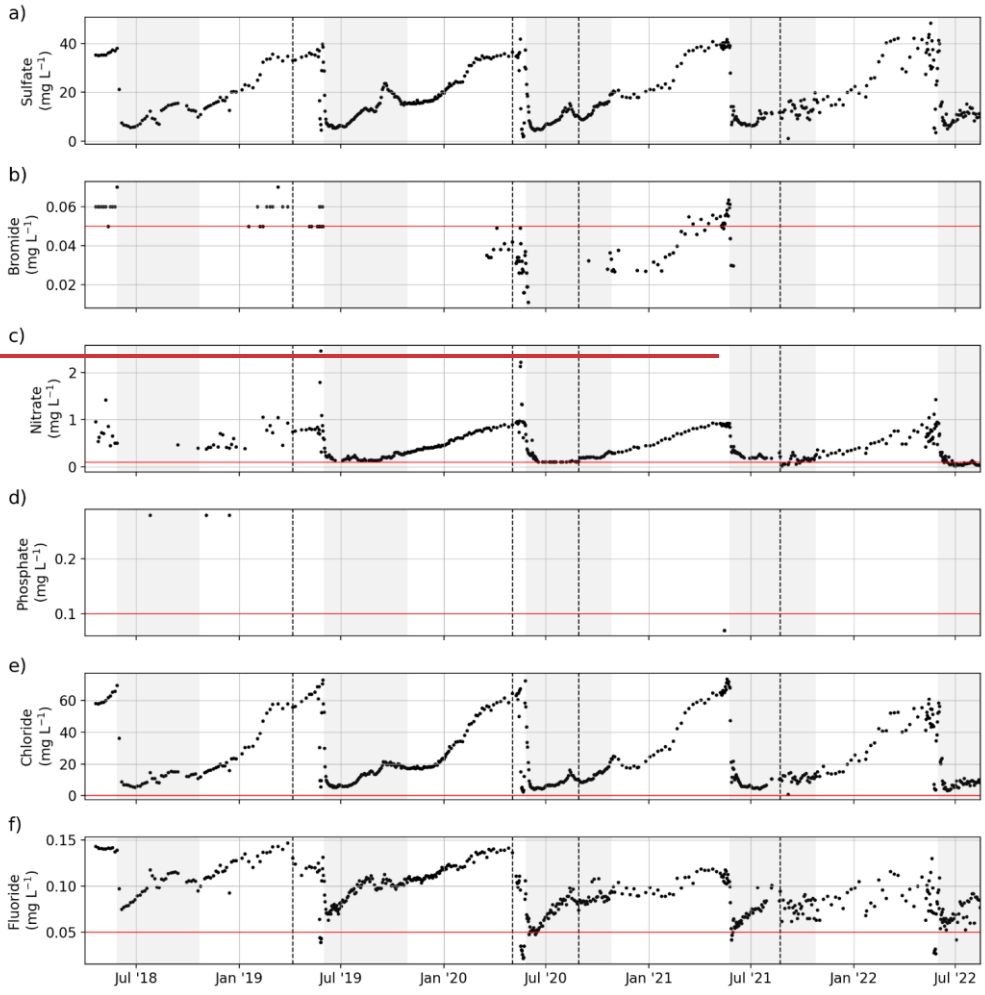
a)
Sulfate (mg L⁻¹)
0
20
40
b)
Bromide (mg L⁻¹)
0.02
0.04
0.06
c)
Nitrate (mg L⁻¹)
0
1
2
d)
Phosphate (mg L⁻¹)
0.1
0.2
e)
Chloride (mg L⁻¹)
0
20
40
60
f)
Fluoride (mg L⁻¹)
0.05
0.10
0.15
Jul '18
Jan '19
Jul '19
Jan '20
Jul '20
Jan '21
Jul '21
Jan '22
Jul '22

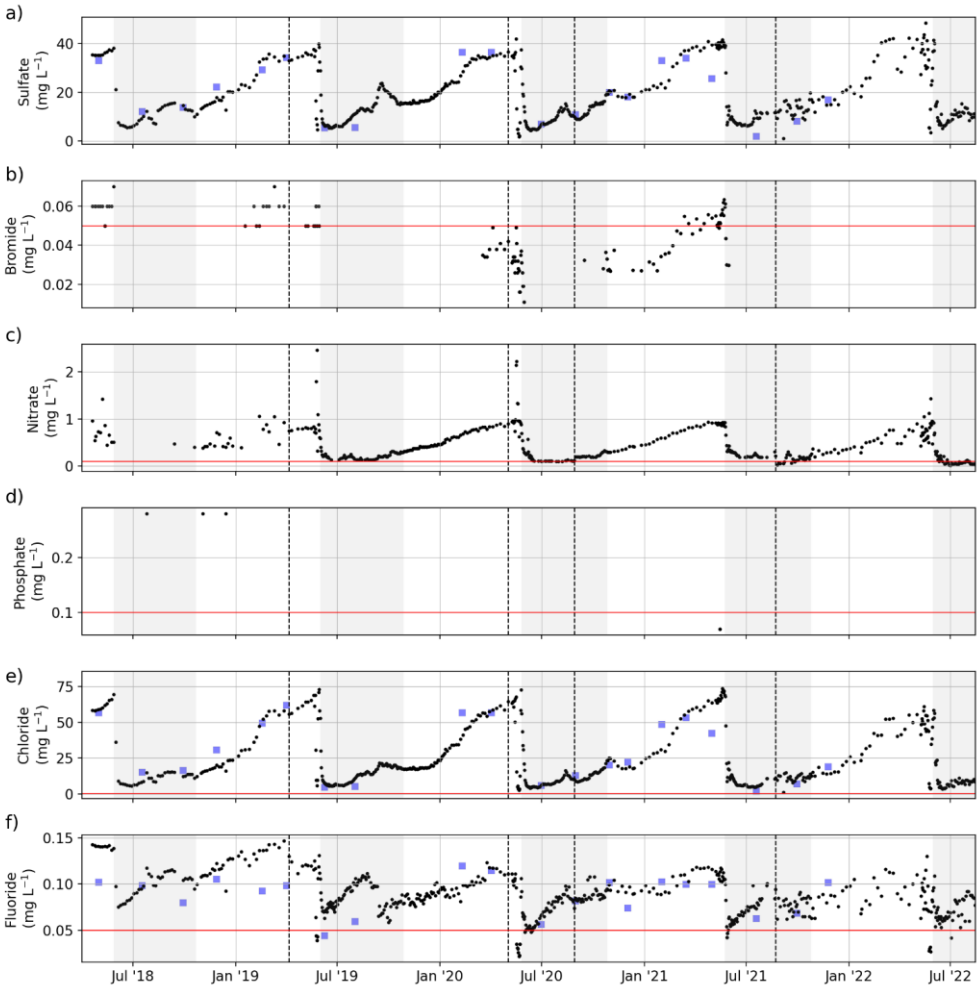

Figure 13: Concentrations of major ions: (a) Si, (b) Br, (c) NO_3, (d) PO_4, (e) Cl, and (f) F. The horizontal red line shows the detection limit. Dashed black lines separate sample sets and indicate a possible change in measurement protocol and method (see Table 1). For comparison, we added data sampled by the ArcticGRO program (blue squares).

In addition, for the samples #001 to #078, the germanium (Ge) concentration and Si isotope composition ($\delta^{30}Si$) was measured (Fig. C1). Heavy metals (Pb, Cr, V, Co, Ni, Cu, Zn) were measured for samples #202 to #487. Concentrations for these

parameters and for all samples were below detection limit, with the exception of some zinc concentrations between 20 and 196 µg L^{-1}.

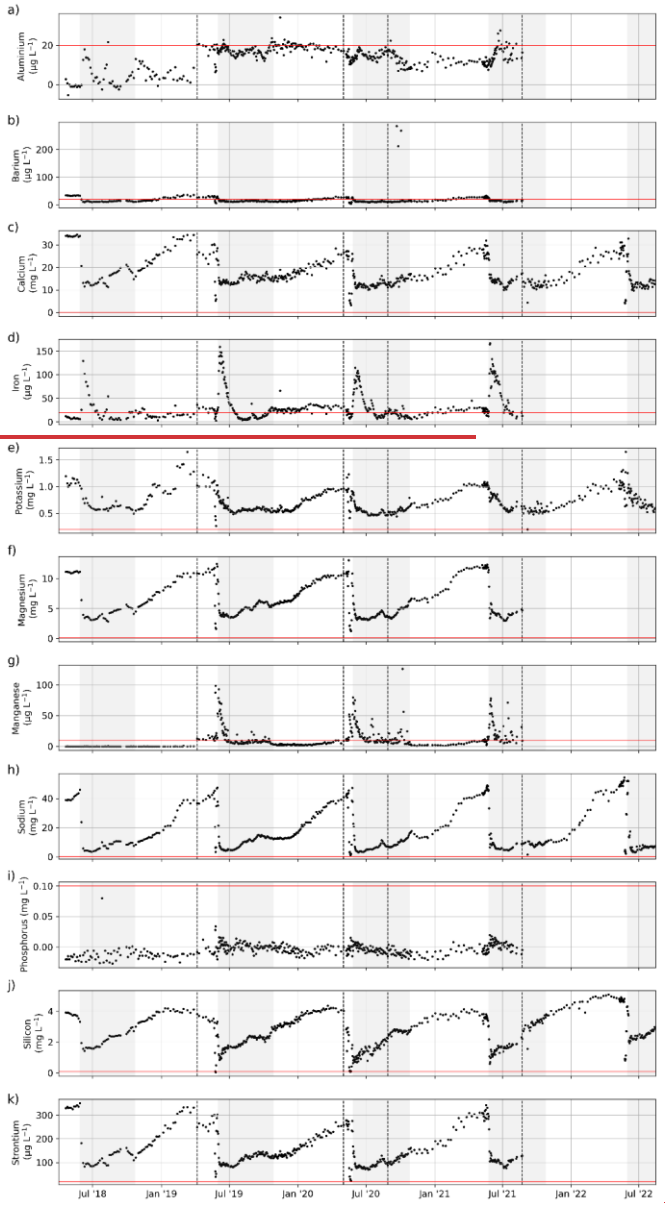
a)
Aluminium (µg L⁻¹)
b)
Barium (µg L⁻¹)
c)
Calcium (mg L⁻¹)
d)
Iron (µg L⁻¹)
e)
Potassium (mg L⁻¹)
f)
Magnesium (mg L⁻¹)
g)
Manganese (µg L⁻¹)
h)
Sodium (mg L⁻¹)
i)
Phosphorus (mg L⁻¹)
j)
Silicon (mg L⁻¹)
k)
Strontium (µg L⁻¹)
Jul '18
Jan '19
Jul '19
Jan '20
Jul '20
Jan '21
Jul '21
Jan '22
Jul '22

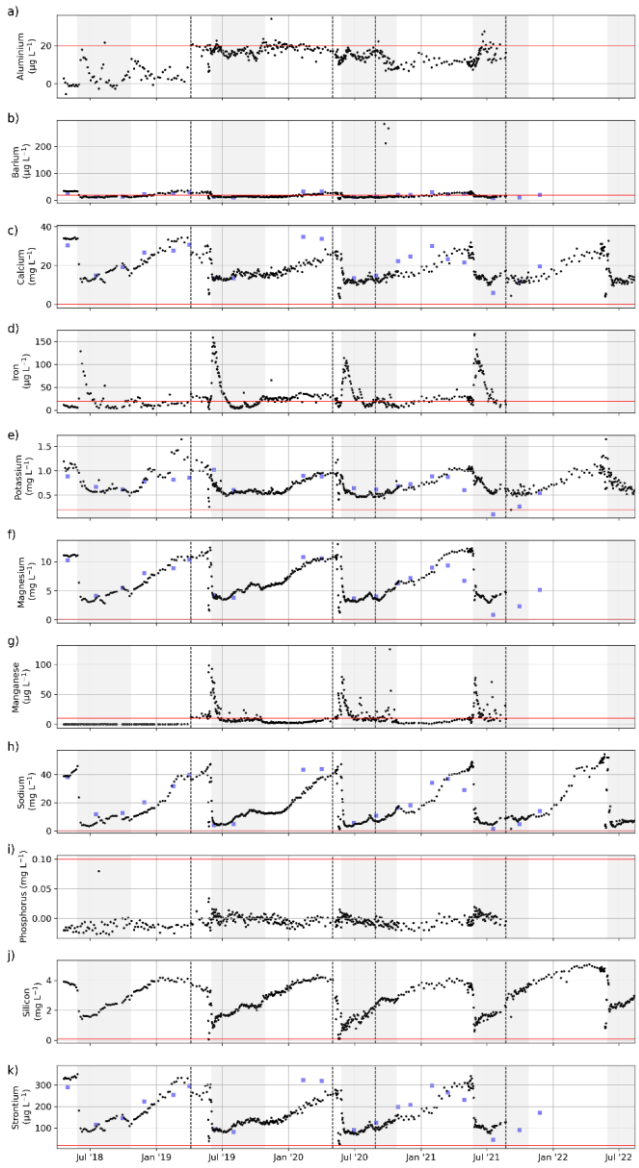
a)
Aluminium (µg L⁻¹)
b)
Barium (µg L⁻¹)
c)
Calcium (mg L⁻¹)
d)
Iron (µg L⁻¹)
e)
Potassium (mg L⁻¹)
f)
Magnesium (mg L⁻¹)
g)
Manganese (µg L⁻¹)
h)
Sodium (mg L⁻¹)
i)
Phosphorus (mg L⁻¹)
j)
Silicon (mg L⁻¹)
k)
Strontium (µg L⁻¹)
Jul '18
Jan '19
Jul '19
Jan '20
Jul '20
Jan '21
Jul '21
Jan '22
Jul '22

Figure 14: Concentrations of total dissolved elemental concentrations: (a) Al, (b) Ba, (c) Ca, (d) Fe, (e) K, (f) Mg, (g) Mn, (h) Na, (i) P, (j) Si, and (k) Sr. The horizontal red line shows the detection limit. Dashed black lines separate sample sets and indicate a possible change in measurement protocol and method (see Table 1). For comparison, we added data sampled by the ArcticGRO program (blue squares).

4 Data availability

The raw data and all related metadata are stored at the Alfred Wegener Institute (AWI), Germany. Final aligned and cleaned datasets are available on Pangaea: https://doi.org/10.1594/PANGAEA.913197 (Juhls et al., 2020b). Detailed metadata are available with digital object identifiers (DOI), including the principal investigator's contact information. Remaining sample volumes of analysed samples are archived at the AWI in Potsdam, Germany. For specific questions, please contact the principal investigator associated with the parameter. In addition, the data from this collection can be explored in an interactive dashboard at https://lena-monitoring.awi.de/.

5 Conclusion

The dataset presented here is the result of a comprehensive, year-round, high-frequency monitoring of the biogeochemistry of the Lena River, covering nearly 4.5 years. The data collection includes a wide range of biogeochemical parameters, maintaining consistency for most parameters in coverage and data quality. This consistency is achieved through the involvement and committed engagement of local partners, simple sampling and sample handling protocols, and effective real-time communication between sampling personnel and scientists. To the best of our knowledge, this data collection represents the most extensive and detailed coverage of an Arctic river's biogeochemistry to date. The high-frequency nature of this dataset is particularly significant, allowing for the observation of biogeochemical changes occurring on a weekly or shorter time scale and justifying interpolation between sampling dates. The high-frequency sampling eliminates the need for gap-filling, e.g. using load models, which ignore flux processes that are independent of discharge. Studies~~,~~ based on this dataset show improved estimates of the loads supplied from terrestrial sources into the Arctic Ocean in terms of both magnitude and timing (Juhls et al., 2020a; Sanders et al., 2022). ~~This dataset~~Specifically the continuous and frequent sampling during winter season ~~also~~ improves the understanding of freezing processes (Lütjen et al., 2024) and the role of the ice-covered period for biogeochemical processing of nutrients in the Lena River prior to their delivery to the Arctic Ocean (Opfergelt et al., accepted~~in review~~). Furthermore, these data serve as a valuable resource for satellite data validation, as demonstrated by El Kassar et al. (2023). Other potential applications of this dataset include enhancing climate and earth system models and supporting policy decisions regarding Arctic environments. This dataset establishes a baseline to monitor future environmental changes across various time scales, from precipitation events to seasonal and interannual variations as well as to detect future changes in river hydrology. Given the current geopolitical situation limiting international access to the Russian Arctic, such robust, long-term datasets will be of great importance to monitor and understand ongoing environmental changes. Using this dataset as a baseline, it should be the goal to repeat such sampling in the future, either as ongoing monitoring, or a repeated intense 4-year period.

Future studies could utilize insights from this high-frequency sampling to determine the optimal sampling frequency needed to address specific scientific questions. Further, to improve inter-lab comparability, we recommend designated tests to measure splits of samples for the same parameters but in different labs and or using different protocols or instruments. Overall, the breadth and quality of this dataset provide an invaluable foundation for future research and monitoring efforts in the rapidly changing Arctic region.

Appendix A

The temperature and electrical conductivity of the entire Lena River water column was measured in different years and seasons (August 2016, March to April and August 2019) at a number of locations in different channels within the Lena River Delta. These profiles show a well-mixed and unstratified water column (**Fig. A1**).

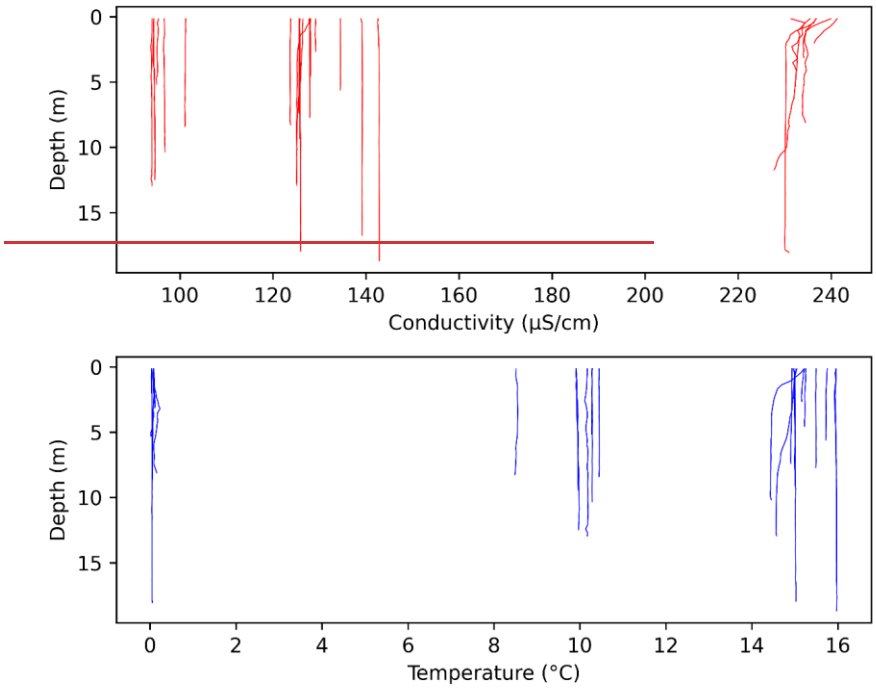
Depth (m)
0
5
10
15
100
120
140
160
180
200
220
240
Conductivity (µS/cm)
Depth (m)
0
5
10
15
0
2
4
6
8
10
12
14
16
Temperature (°C)

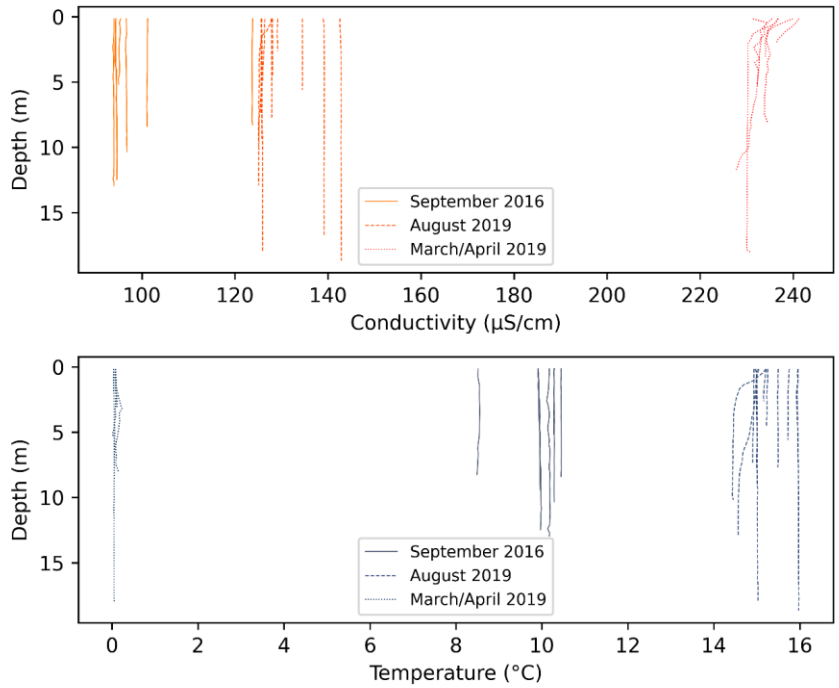

Figure A1: CTD profiles within channels of the Lena River across different years and seasons (https://doi.pangaea.de/10.1594/PANGAEA.933182 and Overduin et al. (2017)).

Appendix B

For a set of samples covering the period from 13 September 2019 to 2 May 2020, we measured the electrical conductivity (Fig. B1), major ion concentrations (Fig. B2), and dissolved elemental concentrations (Fig B3) measured as described in Table 1 but with two different protocols to assess the impact of sample processing on the dissolved elemental and ion concentrations. While some dissolved elemental and ion concentrations show minor differences when comparing the results of the different protocols, some others show large differences or even seasonal differences. For many dissolved elemental and ion concentrations, frozen samples show lower concentrations compared to unfrozen.

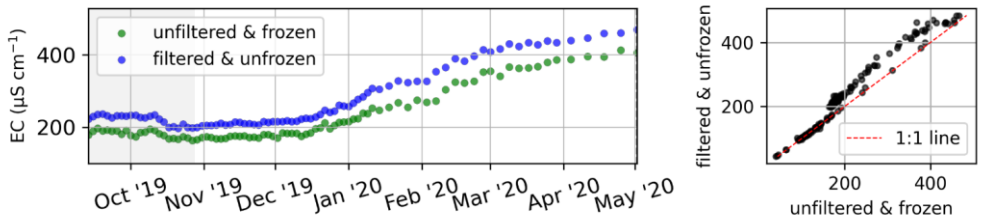

805 **Figure B1: Comparison of electrical conductivity of two sample sets that were processed with two different protocols. One set was frozen right after sampling, then thawed and filtered after storage and transport (green), and the other set was filtered right after sampling and stored and transported unfrozen/cooled (blue). The analysis method for both sets were identical (see Table 1).**

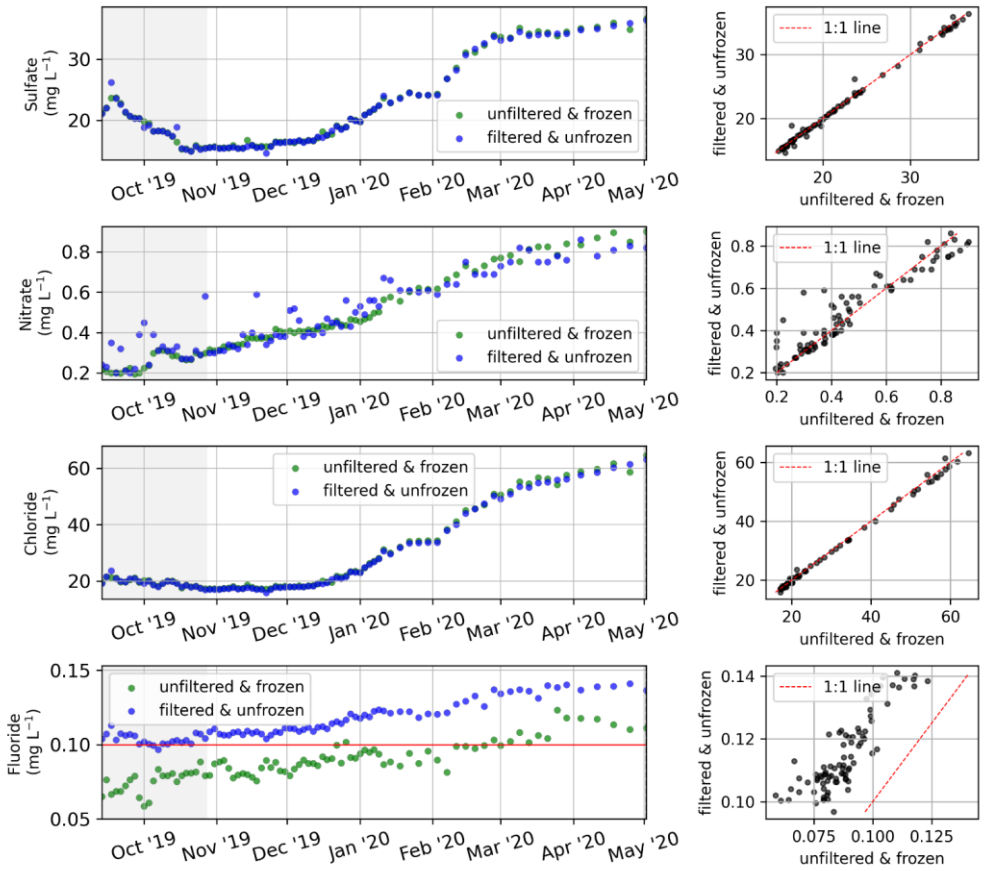

Figure B2: Comparison of major ion concentrations of two sample sets that were processed with two different protocols. One set was frozen right after sampling, then thawed and filtered after storage and transport (green), and the other set was filtered right after sampling and stored and transported unfrozen/cooled (blue). The analysis method for both sets were identical (see Table 1).

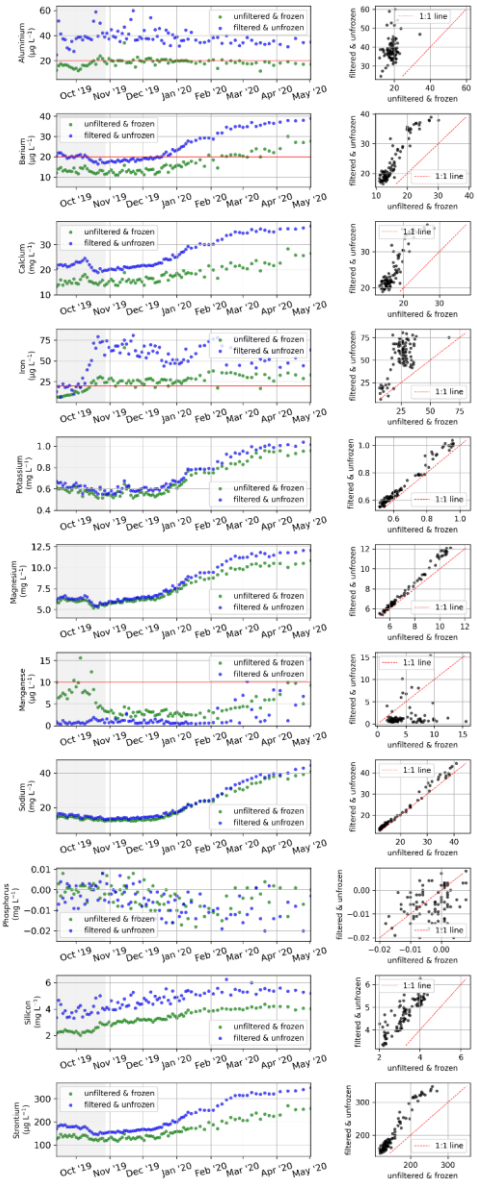
Aluminum (µg L⁻¹)
Barium (µg L⁻¹)
Calcium (mg L⁻¹)
Iron (µg L⁻¹)
Potassium (mg L⁻¹)
Magnesium (mg L⁻¹)
Manganese (µg L⁻¹)
Sodium (mg L⁻¹)
Phosphorus (mg L⁻¹)
Silicon (mg L⁻¹)
Strontium (µg L⁻¹)
unfiltered & frozen
filtered & unfrozen
1:1 line
Oct '19
Nov '19
Dec '19
Jan '20
Feb '20
Mar '20
Apr '20
May '20

Figure B3: Comparison of total dissolved elemental concentrations of two sample sets that were processed with two different protocols. One set was frozen right after sampling, then thawed and filtered after storage and transport (green), and the other set was filtered right after sampling and stored and transported unfrozen/cooled (blue). The analysis method for both sets were identical (see Table 1).

Appendix C

In addition to the parameters shown in the main manuscript, some sample sets or rest volumes of samples were used to measure additional parameters, however, not for the entire period of the sampling program. The germanium (Ge) concentration for samples #001 to #077 (20 April 2018 to 28 March 2019) was determined on rest volumes of the samples for total dissolved elemental concentration by ICP-mass spectrometry (ICP-MS, ICAPQ Thermo Fisher Scientific, Earth & Life Institute, UCLouvain, Belgium). The detection limit for Ge is 0.04 nM and the analytical precision of the measurement is ± 8 % for Ge concentrations < 0.013 nM and ± 4 % for Ge concentrations > 0.013 nM. The silicon isotope composition ($\delta^{30}Si$) was analyzed by MC-ICP-MS (Neptune Plus™ High Resolution Multicollector ICP-MS, Thermo Fisher Scientific, Earth & Life Institute, UCLouvain, Belgium) in wet plasma mode after Si separation using a two-stages column chemistry procedure using an anion exchange resin (Biorad AG MP-1) followed by a cation exchange resin (Biorad AG50W-X12). The instrumental mass bias was corrected using the standard-sample bracketing technique and an external Mg doping. The $\delta^{30}Si$ compositions are expressed in relative deviations of $^{30}Si/^{28}Si$ ratio from the NBS-28 reference standard using the δ-notation (‰) as follows: $\delta^{30}Si = [(^{30}Si/^{28}Si)sample/(^{30}Si/^{28}Si)NBS\text{-}28\ -1] \times 1000$. Each single δ-value represents one sample run and two bracketing standards. The $\delta^{30}Si$ values are reported as the mean of isotopic analyses from multiple analytical sessions at least in duplicate. The long-term precision and accuracy is ± 0.08 ‰ (SD).

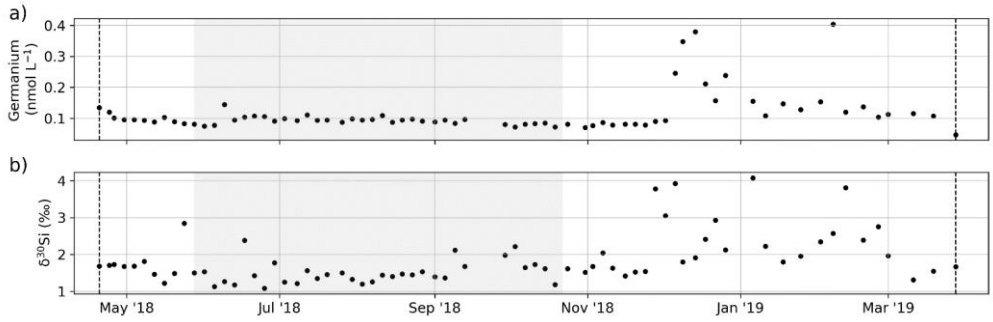

Figure C1: (a) Germanium concentration, (b) dissolved Si isotope composition. Dashed black lines indicate the start and end date of the set of samples that were analyzed.

Organic and inorganic carbon concentrations were measured on unfiltered samples for the period 10 September 2021 to 31 July 2022 (Fig. C2) at the Lomonosov Moscow State University in Moscow, Russia (MSU), using a TOPAZ NC manufactured by Informanalitika LLC (Russia). Analyses for the determination of total carbon concentration are based on ISO 8245 for the

determination of the sum of organically and inorganically bound carbon, including elemental carbon, based on infrared spectrometry of CO_2 after thermocatalytic oxidation of all carbon species. Analyses for the determination of inorganic carbon concentration are based on ISO 8245 for the determination of sum of elemental carbon, carbonates and bicarbonates, carbon dioxide and monoxide, cyanide, cyanate and thiocyanate based on infrared spectrometry of CO_2 after oxidation with phosphoric acid.

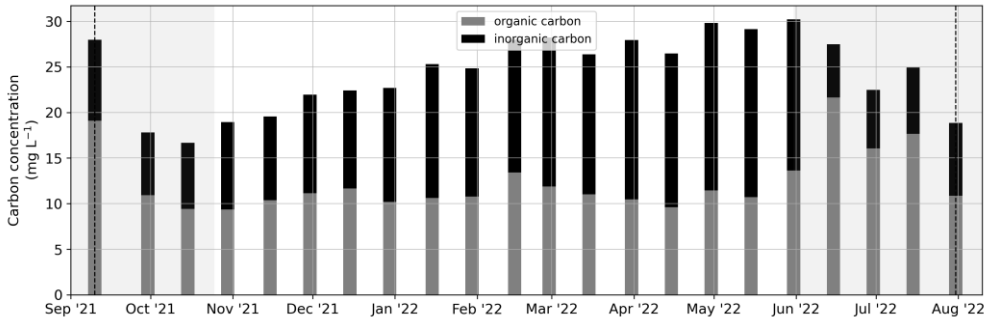

Figure C2: Organic (grey bars) and inorganic carbon (black bars) concentration measured on unfiltered samples that were frozen right after sampling. The sum of organic and inorganic shows the total carbon concentration (top of the stacked bars).

~~Appendix D~~

~~Comparisons to data from the The Arctic Great Rivers Observatory for which the water sampling is conducted in Zhigansk (Fig. 1a), approximately 700 km upstream of the Research Station Samoylov Island.~~

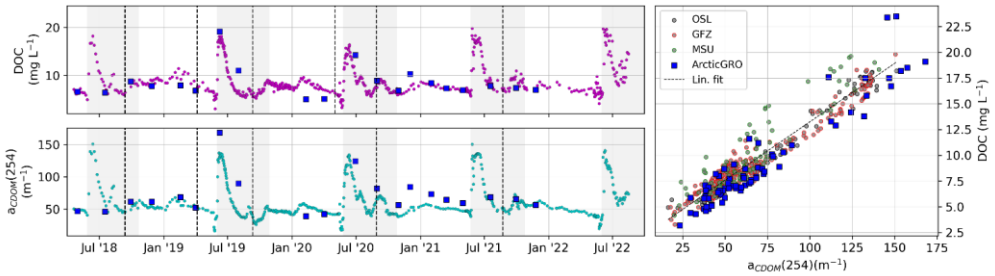

~~**Figure D1: Comparison of DOC concentration and absorption by CDOM at 254 nm with data collected by PARTNERS and ArcticGRO.**~~

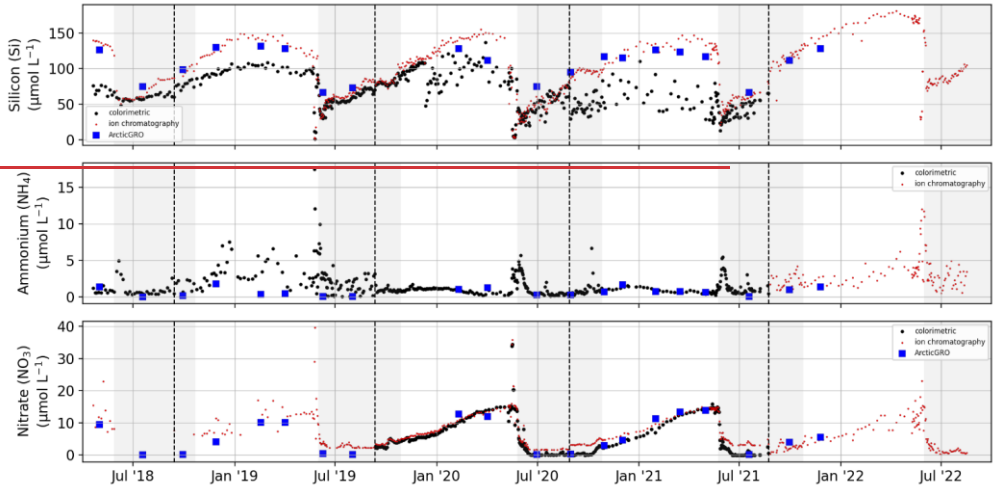

~~**Figure D2: Comparison of Si, NH_4, and NO_3 concentration with data collected by PARTNERS and ArcticGRO.**~~

Author contributions

The research was conceived and coordinated by BJ, AM, and PPO, with initial support from JH and BH. AE was responsible for the preparation of consumables and laboratory analysis of DOC and ions at AWI Potsdam. SA managed program communication and logistics between Russia and Germany. EE, FG, and FM created the data dashboard, processed the data, and ensured quality control. SC, MT, and OE conducted DOC, CDOM, ions, and nutrients measurements at MSU Moscow. Stable oxygen and hydrogen isotope analyses were performed by HM at AWI Potsdam and NT at MPI Yakutsk. Sample and consumables transport in Russia were overseen by GTM, LL, EF, and VP. Sampling was supported by EA, LL, and AC. Nutrient measurements were carried out by TS at Hereon. DOC radiocarbon measurements were performed by HG and GM at AWI Bremerhaven. CDOM and nutrient measurements at OSL, St. Petersburg, were conducted by VP, AC, and JH. Ge and Si isotope measurements were carried out by SO. BJ piloted the creation of figures and tables. BJ wrote the main content of the paper, with further contributions and suggestions from all co-authors.

Competing interests

At least one of the (co-)authors is a member of the editorial board of Earth System Science Data.

Financial support

BJ was supported by the EU Horizon 2020 program (Nunataryuk, grant no. 773421), the European Space Agency (ESA) as part of the Climate Change Initiative (CCI) fellowship (ESA ESRIN/Contract No. 4000l3376l/2l/I-NB) and by the BNP Paribas Foundation Climate & Biodiversity Initiative (project FLO CHAR).~~and by the BNP Paribas Foundation (FLO CHAR Project)~~. Funding for the MICADAS radiocarbon laboratory was provided through AWI institutional core funding and HG was funded by the MARUM Cluster of Excellence "The Oceans Floor – Earth's Uncharted Interface" (DFG Project number 390741603). Funding was provided to SO by the European Research Council (ERC) under the European Union's Horizon 2020 research and innovation programme (WeThaw n°714617) and by the Fonds National de la Recherche Scientifique (FNRS, FC69480). LL, NT and GM were funded by the Melnikov Permafrost Institute SB RAS (project numbers 122012400106-7 and 122011800064-9). SC has been supported by the Kazan Federal University Strategic Academic Leadership Program ("PRIORITY-2030") and Ministry of Science and Higher Education of Russian Federation under the Agreement No 075-15-2024-614. VP was supported by the Federal scientific and technological program for ecological development of the Russian Federation for 2021 - 2030 agreement № 169-03-2024-072.

Acknowledgement

We would like to express our sincere gratitude to the staff of the Research Station Samoylov Island for their central role and expertise in carrying out in situ measurements, water sampling, logistics and communications: Fedor Sellyakhov, Sergey Volkov, Andrey Astapov, and Viktor Zykov. We are grateful to Mikaela Weiner and Andreas Marent at AWI for their work on stable oxygen and hydrogen isotopes. Our appreciation goes to Volkmar Assmann and Waldemar Schneider for their logistical support in Russia through AWI. Special thanks to Pia Esterl, Martha Lütjen, Henrike Walther, Juan Sebastian Valencia Velasquez, and Caroline Herff at AWI for their contributions to sample processing, analysis, and data processing. We acknowledge the administrative and logistical support provided by Mikhail N. Grigoriev at MPI, Yakutsk, Russia and Luidmila Pestryakova at the North-Eastern Federal University in Yakutsk, Russia. We are thankful to Colin Stedmon, Signe Melbye Andersen, and Anders Dalhoff Bruhn Jensen at DTU for their assistance with FDOM measurements. Finally, we extend our gratitude to Elizabeth Bonk, Silla M. Thomsen, and Torben Gentz for their laboratory support at AWI MICADAS. We also extend our thanks to Mathias Bochow and Carsten Neumann at GFZ for their support with CDOM measurements.

References

Aminot, A., Kérouel, R., and Coverly, S. C.: Nutrients in Seawater Using Segmented Flow Analysis, Pract. Guidel. Anal. Seawater, 143–178, https://doi.org/10.1201/9781420073072-12, 2009.

Andersson, C. A. and Bro, R.: The N-way Toolbox for MATLAB, Chemom. Intell. Lab. Syst., 52, 1–4, https://doi.org/10.1016/S0169-7439(00)00071-X, 2000.

The Arctic Great Rivers Observatory: https://www.arcticgreatrivers.org/data.

The Arctic Great Rivers Observatory. 2024. Water Quality Dataset, Version 20241020. https://www.arcticgreatrivers.org/data

Bertin, C., Carroll, D., Menemenlis, D., Dutkiewicz, S., Zhang, H., Matsuoka, A., Tank, S., Manizza, M., Miller, C. E., Babin, M., Mangin, A., and Le Fouest, V.: Biogeochemical River Runoff Drives Intense Coastal Arctic Ocean CO2 Outgassing, Geophys. Res. Lett., 50, e2022GL102377, https://doi.org/10.1029/2022GL102377, 2023.

Biskaborn, B. K., Smith, S. L., Noetzli, J., Matthes, H., Vieira, G., Streletskiy, D. A., Schoeneich, P., Romanovsky, V. E., Lewkowicz, A. G., Abramov, A., Allard, M., Boike, J., Cable, W. L., Christiansen, H. H., Delaloye, R., Diekmann, B., Drozdov, D., Etzelmüller, B., Grosse, G., Guglielmin, M., Ingeman-Nielsen, T., Isaksen, K., Ishikawa, M., Johansson, M., Johannsson, H., Joo, A., Kaverin, D., Kholodov, A., Konstantinov, P., Kröger, T., Lambiel, C., Lanckman, J. P., Luo, D., Malkova, G., Meiklejohn, I., Moskalenko, N., Oliva, M., Phillips, M., Ramos, M., Sannel, A. B. K., Sergeev, D., Seybold, C., Skryabin, P., Vasiliev, A., Wu, Q., Yoshikawa, K., Zheleznyak, M., and Lantuit, H.: Permafrost is warming at a global scale, Nat. Commun., 10, 1–11, https://doi.org/10.1038/s41467-018-08240-4, 2019.

Boss, C. B. and Fredeen, K. J.: Concepts, Instrumentation, and Techniques in Inductively Coupled Plasma Optical Emission Spectrometry, Perkin Elmer, 1997.

Castro-Morales, K., Canning, A., Arzberger, S., Overholt, W. A., Küsel, K., Kolle, O., Göckede, M., Zimov, N., and Körtzinger, A.: Highest methane concentrations in an Arctic river linked to local terrestrial inputs, Biogeosciences, 19, 5059–5077, https://doi.org/10.5194/BG-19-5059-2022, 2022.

Cauwet, G. and Sidorov, I.: The biogeochemistry of Lena River: organic carbon and nutrients distribution, Mar. Chem., 53, 211–227, https://doi.org/10.1016/0304-4203(95)00090-9, 1996.

Chalov, S. R. and Prokopeva, K. N.: Assessment of Suspended Sediment Budget of the Lena River Delta Based on the Remote Sensing Dataset, Izv. - Atmos. Ocean Phys., 57, 1051–1060, https://doi.org/10.1134/S0001433821090450/FIGURES/6, 2021.

Coble, P. G.: Marine Optical Biogeochemistry: The Chemistry of Ocean Color, https://doi.org/10.1021/cr050350, 2007.

Craig, H.: Isotopic variations in meteoric waters, Science (80-.)., 133, 1702–1703, https://doi.org/10.1126/science.133.3465.1702, 1961.

D'Andrilli, J., Silverman, V., Buckley, S., and Rosario-Ortiz, F. L.: Inferring Ecosystem Function from Dissolved Organic Matter Optical Properties: A Critical Review, Environ. Sci. Technol., 56, 11146–11161, https://doi.org/10.1021/ACS.EST.2C04240, 2022.

Fedorova, I., Chetverova, A., Bolshiyanov, D., Makarov, A., Boike, J., Heim, B., Morgenstern, A., Overduin, P. P., Wegner, C., Kashina, V., Eulenburg, A., Dobrotina, E., and Sidorina, I.: Lena Delta hydrology and geochemistry: long-term hydrological data and recent field observations, Biogeosciences, 12, 345–363, https://doi.org/10.5194/bg-12-345-2015, 2015.

Fichot, C. G. and Benner, R.: The spectral slope coefficient of chromophoric dissolved organic matter (S 275-295) as a tracer of terrigenous dissolved organic carbon in river-influenced ocean margins, Limnol. Oceanogr., 57, 1453–1466, https://doi.org/10.4319/lo.2012.57.5.1453, 2012.

Fichot, C. G., Kaiser, K., Hooker, S. B., Amon, R. M. W., Babin, M., Bélanger, S., Walker, S. A., and Benner, R.: Pan-Arctic

distributions of continental runoff in the Arctic Ocean, Sci. Rep., 3, 1053, https://doi.org/10.1038/srep01053, 2013.

Frey, K. E. and Smith, L. C.: Amplified carbon release from vast West Siberian peatlands by 2100, Geophys. Res. Lett., 32, L09401, https://doi.org/10.1029/2004GL022025, 2005.

Gelfan, A., Gustafsson, D., Motovilov, Y., Arheimer, B., Kalugin, A., Krylenko, I., and Lavrenov, A.: Climate change impact on the water regime of two great Arctic rivers: modeling and uncertainty issues, Clim. Change, 141, 499–515, https://doi.org/10.1007/S10584-016-1710-5, 2017.

Hansen, H. P. and Koroleff, F.: Determination of nutrients, Methods Seawater Anal. Third, Complet. Revis. Ext. Ed., 159–228, https://doi.org/10.1002/9783527613984.CH10, 2007.

Helms, J. R., Stubbins, A., Ritchie, J. D., Minor, E. C., Kieber, D. J., and Mopper, K.: Absorption spectral slopes and slope ratios as indicators of molecular weight, source, and photobleaching of chromophoric dissolved organic matter, Limnol. Oceanogr., 53, 955–969, https://doi.org/10.4319/lo.2008.53.3.0955, 2008.

Hölemann, J. A., Schirmacher, M., and Prange, A.: Seasonal variability of trace metals in the Lena River and the southeastern Laptev Sea: Impact of the spring freshet, Glob. Planet. Change, 48, 112–125, https://doi.org/10.1016/J.GLOPLACHA.2004.12.008, 2005.

Holmes, R. M., McClelland, J. W., Peterson, B. J., Tank, S. E., Bulygina, E., Eglinton, T. I., Gordeev, V. V., Gurtovaya, T. Y., Raymond, P. A., Repeta, D. J., Staples, R., Striegl, R. G., Zhulidov, A. V., and Zimov, S. A.: Seasonal and Annual Fluxes of Nutrients and Organic Matter from Large Rivers to the Arctic Ocean and Surrounding Seas, Estuaries and Coasts, 35, 369–382, https://doi.org/10.1007/s12237-011-9386-6, 2012.

Huguet, A., Vacher, L., Relexans, S., Saubusse, S., Froidefond, J. M., and Parlanti, E.: Properties of fluorescent dissolved organic matter in the Gironde Estuary, Org. Geochem., 40, 706–719, https://doi.org/10.1016/j.orggeochem.2009.03.002, 2009.

Juhls, B., Stedmon, C. A., Morgenstern, A., Meyer, H., Hölemann, J., Heim, B., Povazhnyi, V., and Overduin, P. P.: Identifying Drivers of Seasonality in Lena River Biogeochemistry and Dissolved Organic Matter Fluxes, Front. Environ. Sci., 8, 53, https://doi.org/10.3389/FENVS.2020.00053/BIBTEX, 2020a.

Juhls, B., Morgenstern, A., Chetverova, A., Eulenburg, A., Hölemann, J., Povazhnyi, V., and Overduin, P. P.: Lena River surface water monitoring near the Samoylov Island Research Station, https://doi.org/https://doi.pangaea.de/10.1594/PANGAEA.913197, 2020b.

El Kassar, J., Juhls, B., Hieronymi, M., Preusker, R., Morgenstern, A., Fischer, J., and Overduin, P. P.: Optical remote sensing (Sentinel-3 OLCI) used to monitor dissolved organic carbon in the Lena River, Russia, Front. Mar. Sci., 10, https://doi.org/10.3389/FMARS.2023.1082109, 2023.

Knapp, A. N., Sigman, D. M., and Lipschultz, F.: N isotopic composition of dissolved organic nitrogen and nitrate at the Bermuda Atlantic Time-series Study site, Global Biogeochem. Cycles, 19, 1–15, https://doi.org/10.1029/2004GB002320, 2005.

Kothawala, D. N., Murphy, K. R., Stedmon, C. A., Weyhenmeyer, G. A., and Tranvik, L. J.: Inner filter correction of dissolved organic matter fluorescence, Limnol. Oceanogr. Methods, 11, 616–630, https://doi.org/10.4319/LOM.2013.11.616, 2013.

Kutscher, L., Mörth, C. M., Porcelli, D., Hirst, C., Maximov, T. C., Petrov, R. E., and Andersson, P. S.: Spatial variation in concentration and sources of organic carbon in the Lena River, Siberia, J. Geophys. Res. Biogeosciences, 122, 1999–2016, https://doi.org/10.1002/2017JG003858, 2017.

Lara, R. J., Rachold, V., Kattner, G., Hubberten, H. W., Guggenberger, G., Skoog, A., and Thomas, D. N.: Dissolved organic matter and nutrients in the Lena River, Siberian Arctic: Characteristics and distribution, Mar. Chem., 59, 301–309, https://doi.org/10.1016/S0304-4203(97)00076-5, 1998.

Liu, S., Wang, P., Yu, J., Wang, T., Cai, H., Huang, Q., Pozdniakov, S. P., Zhang, Y., and Kazak, E. S.: Mechanisms behind the uneven increases in early, mid- and late winter streamflow across four Arctic river basins, J. Hydrol., 606, 127425, https://doi.org/10.1016/J.JHYDROL.2021.127425, 2022.

Lütjen, M., Overduin, P. P., Juhls, B., Boike, J., Morgenstern, A., and Meyer, H.: Drivers of winter ice formation on Arctic water bodies in the Lena Delta, Siberia, Arctic, Antarct. Alp. Res., 56, https://doi.org/10.1080/15230430.2024.2350546, 2024.

Maie, N., Parish, K. J., Watanabe, A., Knicker, H., Benner, R., Abe, T., Kaiser, K., and Jaffé, R.: Chemical characteristics of dissolved organic nitrogen in an oligotrophic subtropical coastal ecosystem, Geochim. Cosmochim. Acta, 70, 4491–4506, https://doi.org/10.1016/J.GCA.2006.06.1554, 2006.

Mann, P. J., Strauss, J., Palmtag, J., Dowdy, K., Ogneva, O., Fuchs, M., Bedington, M., Torres, R., Polimene, L., Overduin, P., Mollenhauer, G., Grosse, G., Rachold, V., Sobczak, W. V., Spencer, R. G. M., and Juhls, B.: Degrading permafrost river catchments and their impact on Arctic Ocean nearshore processes, Ambio, 51, 439–455, https://doi.org/10.1007/S13280-021-01666-Z, 2022.

McKnight, D. M., Boyer, E. W., Westerhoff, P. K., Doran, P. T., Kulbe, T., and Andersen, D. T.: Spectrofluorometric characterization of dissolved organic matter for indication of precursor organic material and aromaticity, Limnol. Oceanogr., 46, 38–48, https://doi.org/10.4319/lo.2001.46.1.0038, 2001.

Meyer, H., Schönicke, L., Wand, U., Hubberten, H. W., and Friedrichsen, H.: Isotope studies of hydrogen and oxygen in ground ice - Experiences with the equilibration technique, Isotopes Environ. Health Stud., 36, 133–149, https://doi.org/10.1080/10256010008032939, 2000.

Mollenhauer, G., Grotheer, H., Gentz, T., Bonk, E., and Hefter, J.: Standard operation procedures and performance of the MICADAS radiocarbon laboratory at Alfred Wegener Institute (AWI), Germany, Nucl. Instruments Methods Phys. Res. Sect. B Beam Interact. with Mater. Atoms, 496, 45–51, https://doi.org/10.1016/J.NIMB.2021.03.016, 2021.

Murphy, K. R., Stedmon, C. A., Graeber, D., and Bro, R.: Fluorescence spectroscopy and multi-way techniques. PARAFAC, https://doi.org/10.1039/c3ay41160e, 7 December 2013.

Obu, J., Westermann, S., Bartsch, A., Berdnikov, N., Christiansen, H. H., Dashtseren, A., Delaloye, R., Elberling, B., Etzelmüller, B., Kholodov, A., Khomutov, A., Kääb, A., Leibman, M. O., Lewkowicz, A. G., Panda, S. K., Romanovsky, V., Way, R. G., Westergaard-Nielsen, A., Wu, T., Yamkhin, J., and Zou, D.: Northern Hemisphere permafrost map based on TTOP modelling for 2000–2016 at 1 km2 scale, https://doi.org/10.1016/j.earscirev.2019.04.023, 1 June 2019.

Ogneva, O., Mollenhauer, G., Juhls, B., Sanders, T., Palmtag, J., Fuchs, M., Grotheer, H., Mann, P. J., and Strauss, J.:

Particulate organic matter in the Lena River and its delta: from the permafrost catchment to the Arctic Ocean, Biogeosciences, 20, 1423–1441, https://doi.org/10.5194/BG-20-1423-2023, 2023.

Ohno, T.: Fluorescence inner-filtering correction for determining the humification index of dissolved organic matter, Environ. Sci. Technol., 36, 742–746, https://doi.org/10.1021/es0155276, 2002.

Opfergelt, S., Gaspard, F., Hirst, C., Monin, L., Bennet, J., Morgenstern, A., Michael, A., and Overduin, P. P.: Frazil ice changes winter biogeochemical processes in Arctic rivers, Comm Earth Env., 2024.

Overduin, P. P., Blender, F., Bolshiyanov, D., Grigoriev, M., Morgenstern, A., and Meyer, H.: Russian-German Cooperation: Expeditions to Siberia in 2016, in: Berichte zur Polar- und Meeresforschung = Reports on polar and marine research, edited by: Research, A. W. I. for P. and M., Bremerhaven, https://doi.org/doi: 10.2312/BzPM_0709_2017, 2017.

Prokushkin, A. S., Korets, M. A., Panov, A. V., Prokushkina, M. P., Tokareva, I. V., Vorobyev, S. N., and Pokrovsky, O. S.: Carbon and nutrients in the Yenisei River tributaries draining the Western Siberia Peatlands, IOP Conf. Ser. Earth Environ. Sci., 232, 012010, https://doi.org/10.1088/1755-1315/232/1/012010, 2019.

Rachold, V., Alabyan, A., Hubberten, H.-W., Korotaev, V. N., and Zaitsev, A. A.: Sediment transport to the Laptev Sea-hydrology and geochemistry of the Lena River, Polar Res., 15, 183–196, https://doi.org/10.1111/j.1751-8369.1996.tb00468.x, 1996.

Rantanen, M., Karpechko, A. Y., Lipponen, A., Nordling, K., Hyvärinen, O., Ruosteenoja, K., Vihma, T., and Laaksonen, A.: The Arctic has warmed nearly four times faster than the globe since 1979, Commun. Earth Environ. 2022 31, 3, 1–10, https://doi.org/10.1038/s43247-022-00498-3, 2022.

Rawlins, M. A. and Karmalkar, A. V.: Regime shifts in Arctic terrestrial hydrology manifested from impacts of climate warming, Cryosphere, 18, 1033–1052, https://doi.org/10.5194/TC-18-1033-2024, 2024.

Raymond, P. A., McClelland, J. W., Holmes, R. M., Zhulidov, A. V., Mull, K., Peterson, B. J., Striegl, R. G., Aiken, G. R., and Gurtovaya, T. Y.: Flux and age of dissolved organic carbon exported to the Arctic Ocean: A carbon isotopic study of the five largest arctic rivers, Global Biogeochem. Cycles, 21, https://doi.org/10.1029/2007GB002934, 2007.

Sanders, T., Fiencke, C., Fuchs, M., Haugk, C., Juhls, B., Mollenhauer, G., Ogneva, O., Overduin, P., Palmtag, J., Povazhniy, V., Strauss, J., Tuerena, R., Zell, N., and Dähnke, K.: Seasonal nitrogen fluxes of the Lena River Delta, Ambio, 51, 423–438, https://doi.org/10.1007/S13280-021-01665-0, 2022.

Semiletov, I. P., Pipko, I. I., Shakhova, N. E., Dudarev, O. V, Pugach, S. P., Charkin, A. N., McRoy, C. P., Kosmach, D., and Gustafsson, O.: Carbon transport by the Lena River from its headwaters to the Arctic Ocean, with emphasis on fluvial input of terrestrial particulate organic carbon vs. carbon transport by coastal erosion, Biogeosciences, 8, 2407–2426, https://doi.org/10.5194/bg-8-2407-2011, 2011.

Shiklomanov, A., Déry, S., Tretiakov, M., Yang, D., Magritsky, D., Georgiadi, A., and Tang, W.: River freshwater flux to the Arctic ocean, Arct. Hydrol. Permafr. Ecosyst., 703–738, https://doi.org/10.1007/978-3-030-50930-9_24, 2020.

Shiklomanov, A. I. and Lammers, R. B.: River ice responses to a warming Arctic - Recent evidence from Russian rivers, Environ. Res. Lett., 9, https://doi.org/10.1088/1748-9326/9/3/035008, 2014.

Starr, S. F., Frey, K. E., Smith, L. C., Kellerman, A. M., McKenna, A. M., and Spencer, R. G. M.: Peatlands Versus Permafrost: Landscape Features as Drivers of Dissolved Organic Matter Composition in West Siberian Rivers, J. Geophys. Res. Biogeosciences, 129, e2023JG007797, https://doi.org/10.1029/2023JG007797, 2024.

Stuiver, M. and Polach, H. A.: Discussion Reporting of 14C Data, Radiocarbon, 19, 355–363, https://doi.org/10.1017/S0033822200003672, 1977.

Sun, S., Meyer, V. D., Dolman, A. M., Winterfeld, M., Hefter, J., Dummann, W., McIntyre, C., Montluçon, D. B., Haghipour, N., Wacker, L., Gentz, T., Van Der Voort, T. S., Eglinton, T. I., and Mollenhauer, G.: 14C Blank Assessment in Small-Scale Compound-Specific Radiocarbon Analysis of Lipid Biomarkers and Lignin Phenols, Radiocarbon, 62, 207–218, https://doi.org/10.1017/RDC.2019.108, 2020.

Tananaev, N. and Lotsari, E.: Defrosting northern catchments: Fluvial effects of permafrost degradation, Earth-Science Rev., 228, 103996, https://doi.org/10.1016/J.EARSCIREV.2022.103996, 2022.

Tananaev, N. I., Makarieva, O. M., and Lebedeva, L. S.: Trends in annual and extreme flows in the Lena River basin, Northern Eurasia, Geophys. Res. Lett., 43, 10,764-10,772, https://doi.org/10.1002/2016GL070796, 2016.

Tank, S. E., McClelland, J. W., Spencer, R. G. M., Shiklomanov, A. I., Suslova, A., Moatar, F., Amon, R. M. W., Cooper, L. W., Elias, G., Gordeev, V. V., Guay, C., Gurtovaya, T. Y., Kosmenko, L. S., Mutter, E. A., Peterson, B. J., Peucker-Ehrenbrink, B., Raymond, P. A., Schuster, P. F., Scott, L., Staples, R., Striegl, R. G., Tretiakov, M., Zhulidov, A. V., Zimov, N., Zimov, S., and Holmes, R. M.: Recent trends in the chemistry of major northern rivers signal widespread Arctic change, Nat. Geosci. 2023 169, 16, 789–796, https://doi.org/10.1038/s41561-023-01247-7, 2023.

Terhaar, J., Lauerwald, R., Regnier, P., Gruber, N., and Bopp, L.: Around one third of current Arctic Ocean primary production sustained by rivers and coastal erosion, Nat. Commun. 2021 121, 12, 169, https://doi.org/10.1038/s41467-020-20470-z, 2021.

Vonk, J. E., Tank, S. E., and Walvoord, M. A.: Integrating hydrology and biogeochemistry across frozen landscapes, https://doi.org/10.1038/s41467-019-13361-5, 1 December 2019.

Wacker, L. and Christl, M.: Data reduction for small radiocarbon samples: Error propagation using the model of constant contamination, Ion Beam Physics, ETH Zurich, Annu. Rep. 2011, 200, 36, 2011.

Wacker, L., Fahrni, S. M., Hajdas, I., Molnar, M., Synal, H. A., Szidat, S., and Zhang, Y. L.: A versatile gas interface for routine radiocarbon analysis with a gas ion source, Nucl. Instruments Methods Phys. Res. Sect. B Beam Interact. with Mater. Atoms, 294, 315–319, https://doi.org/10.1016/J.NIMB.2012.02.009, 2013.

Weishaar, J. L., Aiken, G. R., Bergamaschi, B. A., Fram, M. S., Roger, F., and Mopper, K.: Evaluation of Specific Ultraviolet Absorbance as an Indicator of the Chemical Composition and Reactivity of Dissolved Organic Carbon, https://doi.org/10.1021/ES030360X, 2003.

Weiss, J.: Ionenchromatographie, Wiley, https://doi.org/10.1002/9783527625031, 2001.

Wild, B., Andersson, A., Bröder, L., Vonk, J., Hugelius, G., McClelland, J. W., Song, W., Raymond, P. A., and Gustafsson, Ö.: Rivers across the Siberian Arctic unearth the patterns of carbon release from thawing permafrost., Proc. Natl. Acad. Sci. U. S. A., 116, 10280–10285, https://doi.org/10.1073/pnas.1811797116, 2019.

Winterfeld, M., Laepple, T., and Mollenhauer, G.: Characterization of particulate organic matter in the Lena River delta and adjacent nearshore zone, NE Siberia - Part I: Radiocarbon inventories, Biogeosciences, 12, 3769–3788, https://doi.org/10.5194/BG-12-3769-2015, 2015.

Wünsch, U. J., Murphy, K. R., and Stedmon, C. A.: Fluorescence quantum yields of natural organic matter and organic compounds: Implications for the fluorescence-based interpretation of organic matter composition, Front. Mar. Sci., 2, 98, https://doi.org/10.3389/FMARS.2015.00098, 2015.

Yang, D., Kane, D. L., Hinzman, L. D., Zhang, X., Zhang, T., and Ye, H.: Siberian Lena River hydrologic regime and recent change, J. Geophys. Res. Atmos., 107, ACL 14-1-ACL 14-10, https://doi.org/10.1029/2002JD002542, 2002.

Zsolnay, A., Baigar, E., Jimenez, M., Steinweg, B., and Saccomandi, F.: Differentiating with fluorescence spectroscopy the sources of dissolved organic matter in soils subjected to drying, Chemosphere, 38, 45–50, https://doi.org/10.1016/S0045-6535(98)00166-0, 1999.

Zsolnay, Á.: Dissolved organic matter: artefacts, definitions, and functions, Geoderma, 113, 187–209, https://doi.org/10.1016/S0016-7061(02)00361-0, 2003.